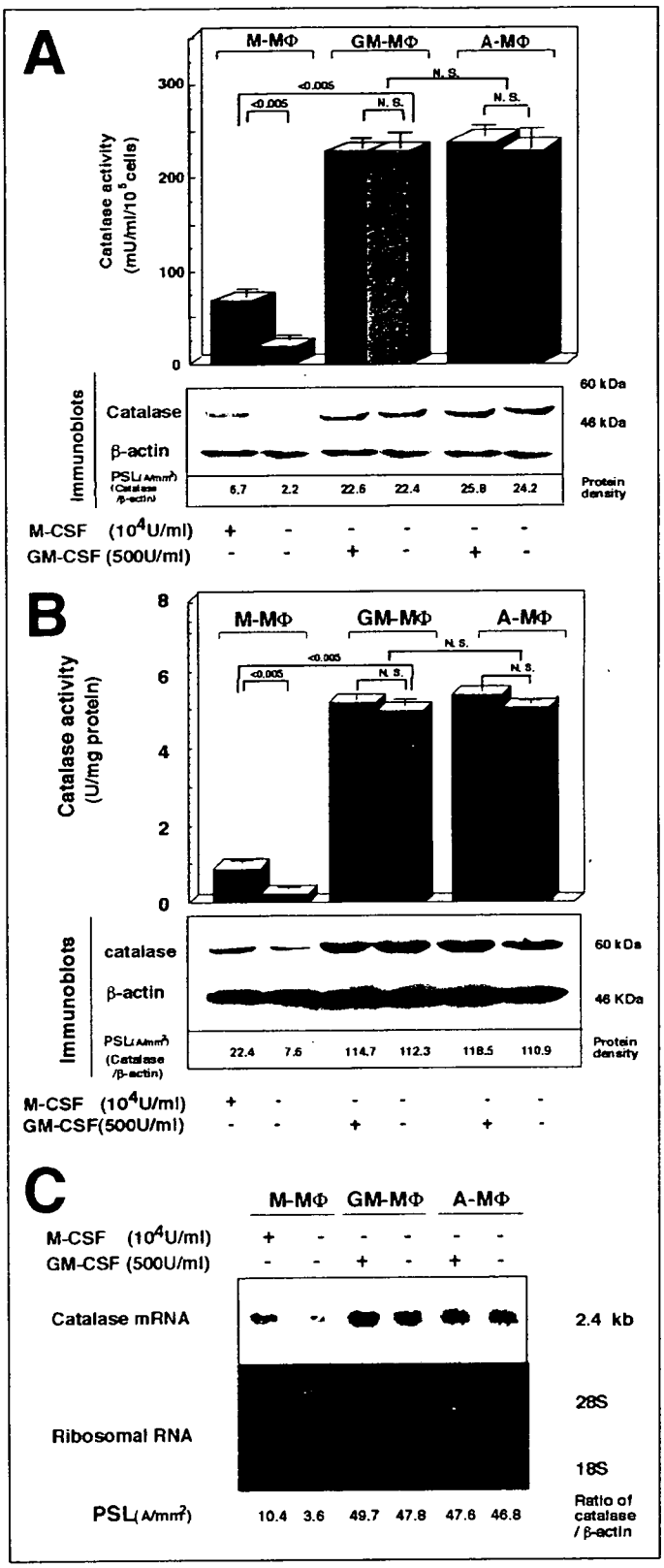

FIGURE 4. **Activities, protein levels, and mRNA levels of catalase in monocyte-derived MΦ and A-MΦ.** MΦ were cultured with or without CSF for 48 h (*A*, *B*) or for 3 h (*C*). *A* and *B*, enzyme activities (*upper panel*) and protein levels (*lower panel*) of catalase in the culture medium (25 μl/lane) (*A*) or cell lysates (25 μg/lane) (*B*) from MΦ were examined as described under "Experimental Procedures." Western blot analysis of catalase protein in the culture medium or cell lysates of MΦ was performed using anti-catalase antibody. The relative amounts of catalase protein in cells were measured using NIH image software, and the expression levels were corrected relative to those of β-actin (photo-stimulating luminescence (*PSL*), A/mm²). *C*, mRNA levels of catalase and the β-actin gene were examined in total RNA preparations (10 μg/lane) from these MΦ at 3 h of cultivation by Northern blot analysis. The relative transcript levels of catalase mRNA in cells were measured using NIH image software, and the expression levels were corrected relative to those of β-actin (photo-stimulating luminescence, A/mm²).

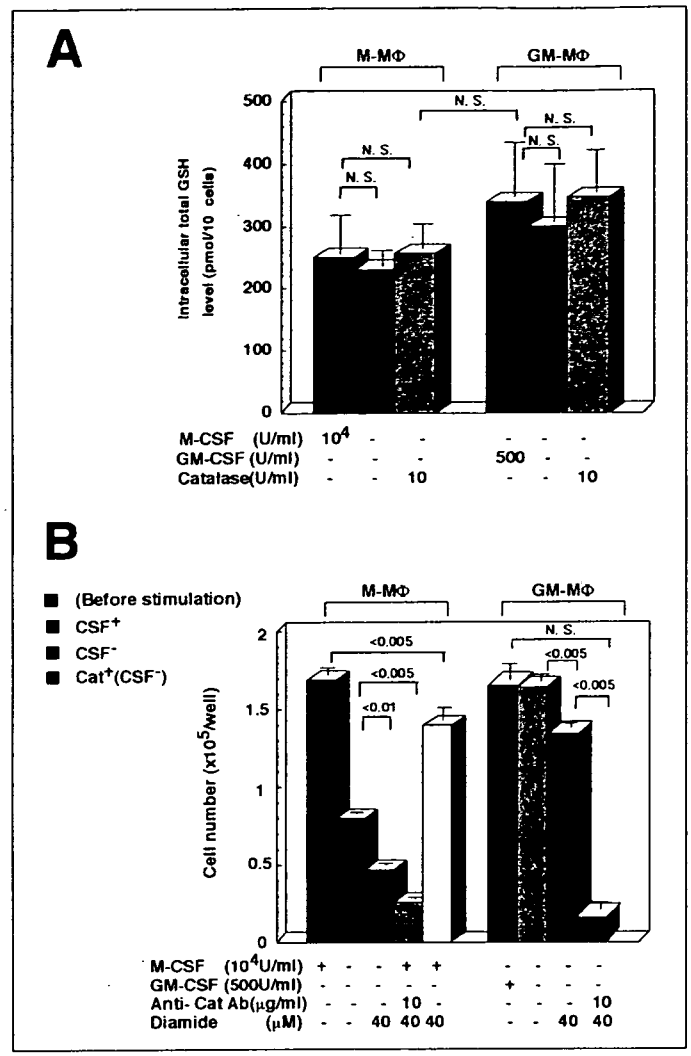

FIGURE 5. **Partial effect of GSH on the survival of monocyte-derived MΦ.** *A*, intracellular GSH levels in M-MΦ and GM-MΦ incubated with or without CSF for 24 h were measured as described under "Experimental Procedures." Values are expressed as the means of triplicate cultures ± S.D. *B*, M-MΦ or GM-MΦ were cultured for 48 h in medium supplemented or not supplemented with CSF, anti-catalase antibody (*Anti-Cat Ab*), diamide, or the combination of them, and cell number and viability were assessed as described above.

lymphocytes or neuronal cells in the absence of growth factors (22, 23, 24). Thus, thiol derivatives may help MΦ survival. The level of intracellular GSH, however, was almost the same in M-MΦ and GM-MΦ cultured with or without CSF or cultured with catalase (Fig. 5*A*), and this level (~300 pmol/10^5 cells) was similar to that in A-MΦ (data not shown). Diamide, which can bind the SH groups of reduced thiols and oxidize them (22), induced cell death of M-MΦ and GM-MΦ, but the levels of cell death were not very high (~20%) and no significant difference was observed between the effects of diamide on these two MΦs (Fig. 5*B*). 40 μM diamide and 10 μg/ml anti-Cat Ab showed synergistic effects on the cell viability of M-MΦ cultured with M-CSF and GM-MΦ cultured without CSF, causing reduction of their viability to <10% at 48 h (Fig. 5*B*). These results suggest that, in contrast to that of catalase,

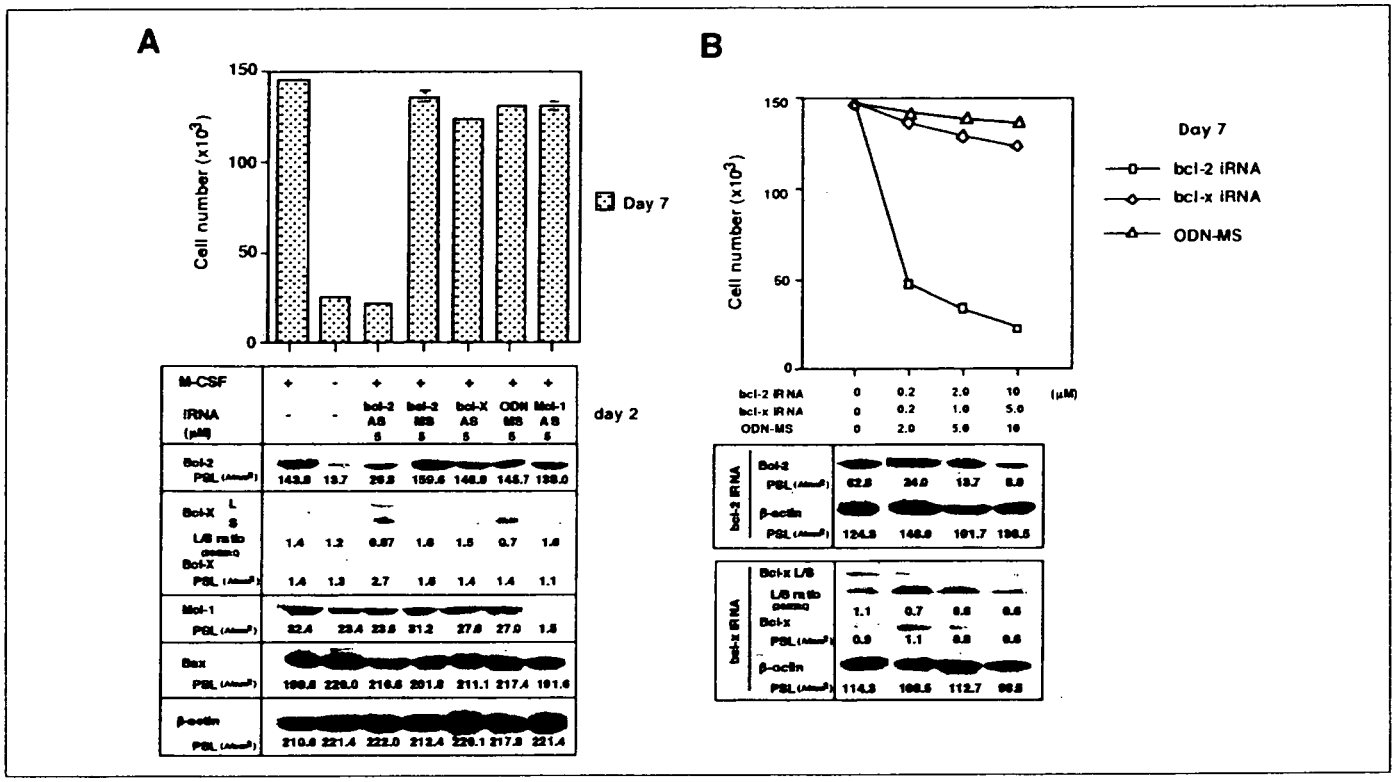

FIGURE 6. **BCL-2 AS dominantly induced cell death of M-MΦ.** *A*, cell number and viability of MΦ at 7 days after 5 μM AS treatment (*upper panel*) and immunoblot analysis at 2 days (*lower panel*). *B*, cell number and viability of MΦ at 7 days after the indicated concentrations of AS treatment (*upper panel*) and immunoblot analysis at 2 days (*lower panel*). M-MΦ were cultured in medium supplemented with the indicated concentrations of BCL-2 AS (G3139), BCL-2 MS (G4126), 5′-BCL-X AS (BCL-X AS), MCL-AS or control random sequence (oligonucleotide MS). Cell number and viability of MΦ were assessed as described in Fig. 1. Values are expressed as the means of triplicate cultures ± S.D. Western blot analysis of BCL-2, BCL-$X_{L/S}$, MCL-1, and β-actin proteins in cell lysates of MΦ probed using BCL-2, BCL-X (antibody from Santa Cruz Biotechnology for $X_{L/S}$ band, from Sinal transduction Labo for X_L band only), and β-actin antibody was performed as described in Fig. 4. The relative amounts of these proteins in cells were measured using NIH image software, and the expression levels were shown as photo-stimulating luminescence (*PSL*).

the levels of thiol derivatives were constant in these MΦs with CSF withdrawal-induced oxidative stress and that thiol derivatives have only a minor effect and cannot support the full survival of MΦ.

BCL-2 AS and BCL-X_L AS Dominantly Induce Cell Death of M-MΦ and GM-MΦ, Respectively—M-MΦ and GM-MΦ were treated with BCL-2 AS targeted to *BCL-2* initiation codon (G3139) and 5′-BCL-X AS targeted to the downstream alternative 5′-splice site of exon 2 of the *BCL-X* gene (12, 13). As controls, these MΦs were treated with BCL-2 MS (G4126, variant G3139), control oligonucleotides with random sequence (oligonucleotide MS), or Lipofectin alone. As shown in Fig. 6, BCL-2 AS (G3139) down-regulated the expression of BCL-2 protein in M-MΦ to 10–20% of that of control cells at 2 days after the oligonucleotide treatment and induced cell death in a dose-dependent manner. The cell viability markedly decreased to ~15% of that of control cells at 7 days of cultivation. In GM-MΦ, however, treatment with G3139 even in the high dose such as 10 μM induced only ~10% cell death, in agreement with the low expression of BCL-2 protein in this MΦ (Fig. 7).

In contrast, treatment of GM-MΦ with 5′-BCL-X AS down-regulated the expression of BCL-X_L protein to 20% of that of control cells treated with oligonucleotide MS at 2 days after the oligonucleotide treatment and induced the cell death in a dose-dependent manner (Fig. 7). The cell viability markedly decreased to ~25% of that of control cells at 7 days of cultivation. As shown in Fig. 6, however, ~90% of the cells are viable in M-MΦ treated with 5 mM 5′-BCL-X AS in agreement with the low expression of BCL-X_L protein.

MCL-1, a main molecule of BCL-2 family protein (14), is expressed in both M-MΦ and GM-MΦ, but down-regulation of this protein by treatment with MCL-1 AS did not stimulate the cell death of either MΦ or affect the expression levels of BCL-2 in M-MΦ and BCL-X_L in GM-MΦ. These findings suggest that BCL-2 and BCL-X_L expression supported by catalase prevents cell death of M-MΦ and GM-MΦ, respectively, in agreement with the dominant expression levels of gene and protein of BCL-2 in M-MΦ and BCL-X_L in GM-MΦ.

DISCUSSION

The present study showed that extracellular catalase has a novel role in the prevention of apoptosis in human MΦ through the dominant expression of BCL-2 in M-MΦ and BCL-X_L in GM-MΦ and that the regulation of catalase production is CSF-dependent in M-MΦ but CSF-independent in GM-MΦ and A-MΦ. Recently, H_2O_2 has been shown to enhance oxidative damage and apoptosis in C2-ceramide-pretreated HL-60 cells via a mechanism in which C2-ceramide inhibits catalase activity by increasing casapase-3-dependent proteolysis of catalase and down-regulation of catalase mRNA (25). Overexpression of catalase inhibits oxidation-mediated apoptosis through phosphorylated BCL-2, a reduced form of BCL-2 and BAX interaction (20). Thus, constant high activity of extracellular catalase plays an important role in the prevention of ceramide- and caspase-3-induced apoptosis in CSF independent of GM-MΦ and A-MΦ and CSF dependent of M-MΦ (11, 26).

GM-CSF and M-CSF stimulate catalase induction during the differentiation of Mo into MΦ, but GM-CSF alone establishes a CSF-independent autoregulatory system of catalase production in MΦ. We previously showed that human Mo-derived GM-MΦ resembles human A-MΦ in several respects (2, 5–7). In this study, we showed that GM-MΦ and A-MΦ have a similar phenotype of the resistance to apoptosis via CSF-independent expression of catalase and BCL-X_L. Con-

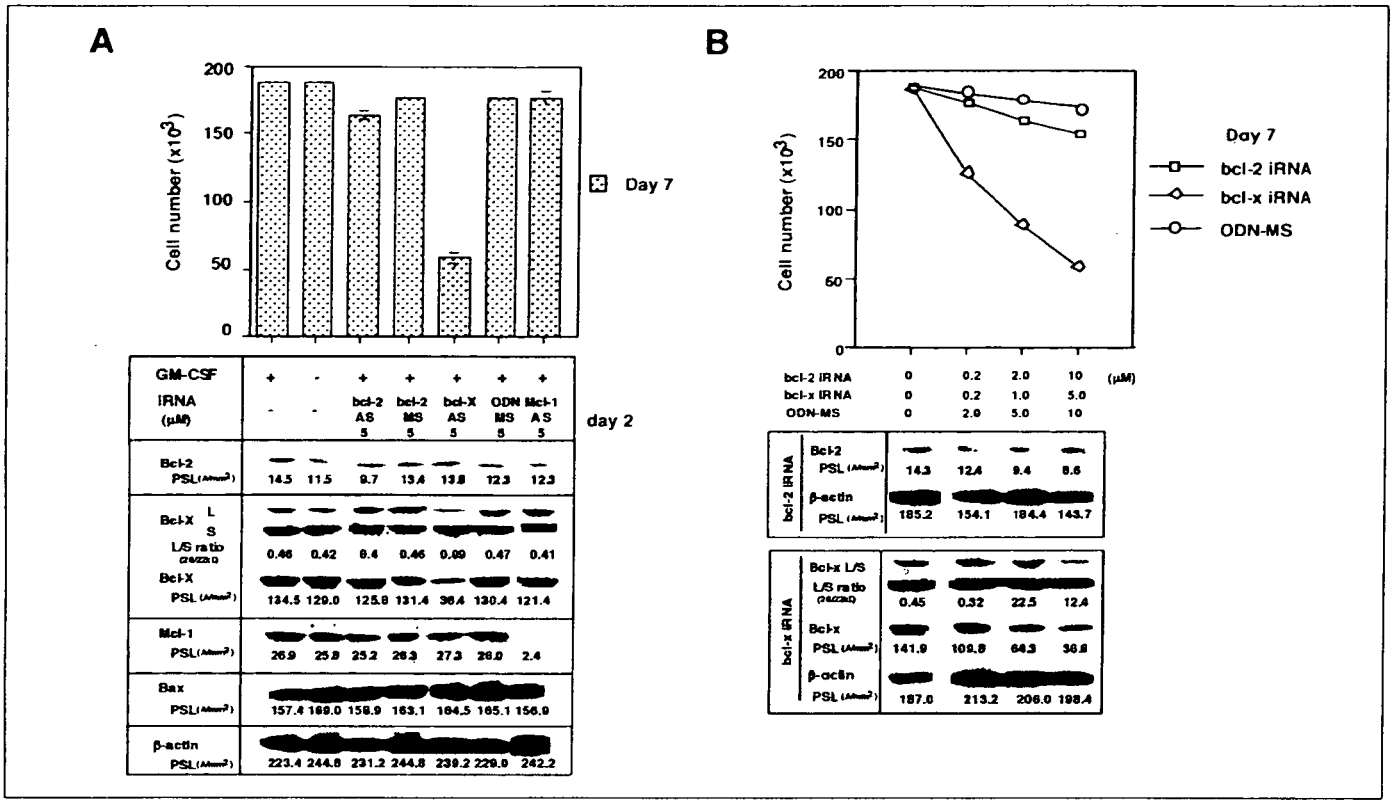

FIGURE 7. **BCL-X AS dominantly induced cell death of GM-MΦ.** *A*, cell number and viability of MΦ at 7 days after 5 μM AS treatment (*upper panel*) and immunoblot analysis at 2 days (*lower panel*). *B*, cell number and viability of MΦ at 7 days after the indicated concentrations of AS treatment (*upper panel*) and immunoblot analysis at 2 days (*lower panel*). The experimental procedure was performed as described in Fig. 6.

sistent with our present study, A-MΦ from human smokers express higher levels of $p21^{CIP1/WAF1}$ and BCL-X_L, but not BCL-2, and the former two molecules may reduce apoptosis (9). The autoregulatory mechanism of catalase induction in GM-MΦ and A-MΦ is not yet understood but may have a strong correlation with endogenously generated low levels of H_2O_2 (8), because we previously showed that GM-MΦ and A-MΦ, but not M-MΦ, can increase catalase expression at both the protein and mRNA levels when stimulated with H_2O_2 (2). Adequate low levels of H_2O_2 may keep catalase activity constant to prevent CSF deprivation-induced apoptosis in GM-MΦ and A-MΦ.

Thiol derivatives such as GSH, adult T cell leukemia-derived factor, and L-cysteine play an important role in the survival of lymphocytes or neuronal cells in the absence of growth factors (22–24). In our study, however, the activity of thiol derivatives was not significantly different between M-MΦ and GM-MΦ before and after CSF deprivation, and they had only a partial effect on MΦ survival. The reason for the differences between our study and previous studies might have been the differences in the experimental conditions (CSF-withdrawal *versus* serum depletion) or the cell type examined (MΦ *versus* lymphocytes/neuronal cells). Compared with MΦ, lymphocytes or neuronal cells may produce lower levels of catalase so that the thiol derivatives play a dominant role in their survival (21–24).

We demonstrated that catalase regulates apoptosis through the expression of BCL-2 and BCL-X_L in human MΦ used in the present study. In fact, down-regulation of these proteins by RNA interference treatment induced the cell death of the MΦs. Proapoptotic BCL-2 family protein, BAX, can induce apoptosis with permeabilization of mitochondrial membranes and cytochrome *c* release (10, 18, 27). In a recent study, induction of apoptosis of TF-1 cells by GM-CSF withdrawal is shown to be related to down-regulation of the *MCL-1* gene, and overexpression of *MCL-1* is shown to delay apoptosis (16). In our study, however, *BAX* and *MCL-1* were not associated with the regulation of apoptosis of MΦ, because both mRNA and protein levels of these genes were not significantly changed in M-MΦ and GM-MΦ after CSF deprivation. Moreover, we showed that down-regulation of the expression of MCL-1 protein by MCL-1 As treatment did not affect the viability of the MΦs.

Our interesting finding is that BCL-2 and BCL-X_L are differently expressed in MΦ during the Mo differentiation into MΦ in the presence of M-CSF and GM-CSF; the expression of BCL-2 is dominant in M-MΦ and that of BCL-X_L is dominant in GM-MΦ or A-MΦ. In accordance with such different expression patterns, we found by RNA interference experiments that BCL-2 and BCL-X_L play a critical role for the survival of M-MΦ and GM-MΦ, respectively. Similar differential expression of BCL-2 and BCL-X_L is also observed during the selection and maturation of mouse thymocytes toward splenic T cells (17, 19). At present, we do not know the mechanisms that control the different induction of BCL-2 and BCL-X_L in M-MΦ and GM-MΦ or A-MΦ, respectively. The distal promoter region of the BCL-X_L gene responds to very low levels of H_2O_2 at exon 1B-1D in rodent cardiac myocytes, and the expression of BCL-X_L protein is increased by H_2O_2 treatment (28). Thus, GM-MΦ and A-MΦ, which possess high catalase activity even in the absence of CSF, limit the levels of endogenously generated H_2O_2 to low levels that are suitable for BCL-X_L expression.

In conclusion, the present study is the first to reveal that CSF is a critical regulator of extracellular catalase activity that maintains selective expression of *BCL-2* family genes and prevents tissue-specific MΦ from apoptosis. These distinct patterns of CSF-induced regulation of catalase activity may greatly contribute to the oxidant stress-induced selection of tissue MΦs suitable for their respective microenvironments.

REFERENCES

1. Pietarinen, P., Raivio, K., Devlin, R. B., Crapo, J. D., Chang, L. Y., and Kinnula, V. L. (1995) *Am. J. Respir. Cell Mol. Biol.* **13,** 434–441
2. Komuro, I., Keicho, N., Iwamoto, A., and Akagawa, K. S. (2001) *J. Biol. Chem.* **276,** 24360–24364
3. Eischen, A., Duclos, B., Schmitt-Goguel, M., Rouyer, N., Bergerat, J. P., Hummel, M., Oskam, R., and Oberling, F. (1994) *Br. J. Haematol.* **88,** 712–722
4. Dranoff, G., Crawford, A. D., Sadelain, M., Ream, B., Rashid, A., Bronson, R. T., Dickersin, G. R., Bachurski, C. J., Mark, E. L., Whitsett, J. A., and Mulligan, R. C. (1994) *Science* **264,** 713–716
5. Hashimoto, S. I., Komuro, I., Yamada, M., and Akagawa, K. S. (2001) *J. Immunol.* **167,** 3619–3625
6. Akagawa, K. S. (2002) *Int. J. Hematol.* **76,** 27–34
7. Komuro, I., Yokota, Y., Yasuda, S., Iwamoto, A., and Kagawa, K. S. (2003) *J. Exp. Med.* **198,** 443–453
8. Borutaite, V., and Brown, G. C. (2001) *FEBS Lett.* **500,** 114–118
9. Tomita, K., Caramori, G., Lim, S., Ito, K., Hanazawa, T., Oates, T., Chiselita, I., Jazrawi, E., Chung, K. F., Barnes, P. J., and Adcock, I. M. (2002) *Am. J. Respir. Crit. Care Med.* **166,** 724–731
10. Shankaranarayanan, P., and Nigam, S. (2003) *J. Immunol.* **170,** 887–894
11. Goyal, A., Wang, Y., Graham, M. M., Doseff, A. I., Bhatt, N. Y., and Marsh, C. B. (2002) *Am. J. Respir. Cell Mol. Biol.* **26,** 224–230
12. Raffo, A., Lai, C. J., Stein, A. C., Miller, P., Scaringe, S., Khvorova, A., and Benimetskaya, L. (2004) *Clin. Cancer Res.* **10,** 3195–3206
13. Mercatante, R. D., Bortner, D. C., Cidlowski, A. J., and Ryszard, K. (2001) *J. Biol. Chem.* **276,** 16411–16417
14. Derenne, S., Monia, B., Dean, M. N., Taylor, K. J., Rapp, M.-J., Harousseau, J.-L., Bataille, R., and Amiot, M. (2002) *Blood* **100,** 194–199
15. Anderson, M. E. (1989) in *Glutathione: Chemical, Biochemical, and Medical Aspects* (Dolphind, D., Poulson, R., and Avramovic O., eds) Vol. A, 339–365, John Wiley and Sons, New York
16. Liu, H., Ma, Y., Cole, S. M., Zander, C., Chen, K. H., Karras, J., and Pope, R. M. (2003) *Blood* **13,** 13
17. Broome, H. E., Dargan, C. M., Krajewski, S., and Reed, J. C. (1995) *J. Immunol.* **155,** 2311–2317
18. Yamaguchi, H., and Wang, H. G. (2001) *Oncogene* **20,** 7779–7786
19. Haughn, L., Hawley, R. G., Morrison, D. K., Von Boehmer, H., and Hockenbery, D. M. (2003) *J. Biol. Chem.* **28,** 28
20. Xiao, D., Choi, S., Johnson, D. E., Vogel, V. G., Johnson, C. S., Trump, D. L., Lee, Y. J., Singh, S. V., Lu, D., Bai, X. C., Gui, L., Su, Y. C., Deng, F., Liu, B., Li, X. M., Zeng, W. S., Cheng, B. L., Luo, S. Q., Pugazhenthi, S., Nesterova, A., Jambal, P., Audesirk, G., Kern, M., Cabell, L., Eves, E., Rosner, M. R., Boxer, L. M., Reusch, J. E., Liu, A. L., Zou, Z. P., Wang, Y., Ke, Z. Y., and Ji, Q. S. (2004) *Oncogene* **7,** 7
21. Sandstrom, P. A., and Buttke, T. M. (1993) *Proc. Natl. Acad. Sci. U. S. A.* **90,** 4708–4712
22. Sato, N., Iwata, S., Nakamura, K., Hori, T., Mori, K., and Yodoi, J. (1995) *J. Immunol.* **154,** 3194–3203
23. Iwata, S., Hori, T., Sato, N., Hirota, K., Sasada, T., Mitsui, A., Hirakawa, T., and Yodoi, J. (1997) *J. Immunol.* **158,** 3108–3117
24. Kirkland, R. A., and Franklin, J. L. (2001) *J. Neurosci.* **21,** 1949–1963
25. Iwai, K., Kondo, T., Watanabe, M., Yabu, T., Kitano, T., Taguchi, Y., Umehara, H., Takahashi, A., Uchiyama, T., and Okazaki, T. (2003) *J. Biol. Chem.* **278,** 9813–9822
26. Yamada, Y., Kajiwara, K., Yano, M., Kishida, E., Masuzawa, Y., and Kojo, S. (2001) *Biochim. Biophys. Acta* **1532,** 115–120
27. Garland, J. M., and Rudin, C. (1998) *Blood* **92,** 1235–1246
28. Valks, D. M., Kemp, T. J., and Clerk, A. (2003) *J. Biol. Chem.* **278,** 25542–25547

Respirology (2006) **11**, S32–S36

Functional heterogeneity of colony-stimulating factor-induced human monocyte-derived macrophages

KIYOKO S. AKAGAWA,[1] IWAO KOMURO,[1] HIROKO KANAZAWA,[1] TOSHIO YAMAZAKI,[2] KEIKO MOCHIDA[3] AND FUMIO KISHI[4]

[1]*Department of Immunology,* [2]*Department of Bacteriology,* [3]*Department of Bacterial Pathogenesis and Infection Control, National Institute of Infectious Diseases, Tokyo, and* [4]*Department of Molecular Genetics, Kagoshima University Graduate School of Medical and Dental Sciences, Kagoshima, Japan*

Functional heterogeneity of colony-stimulating factor-induced human monocyte-derived macrophages
AKAGAWA KS, KOMURO I, KANAZAWA H, YAMAZAKI T, MOCHIDA K, KISHI F. *Respirology* 2006; **11**: S32–S36

Objectives: Macrophages (Mφs) have various functions and play a critical role in host defense and the maintenance of homeostasis. Mφs exist in every tissue in the body, but Mφs from different tissues exhibit a wide range of phenotypes with regard to their morphology, cell surface antigen expression and function, and are called by different names. However, the precise mechanism of the generation of macrophage heterogeneity is not known. In the present study, the authors examined the functional heterogeneity of Mφs generated from human monocytes under the influence of granulocyte-macrophage colony-stimulating factor (GM-CSF) and macrophage-CSF (M-CSF).

Methodology: CD14 positive human monocytes (Mos) were incubated with M-CSF and GM-CSF for 6–7 days to stimulate the generation of M-CSF-induced monocyte-derived Mφs (M-Mφs) and GM-CSF-induced monocyte-derived Mφs (GM-Mφs), respectively. The expression of cell surface antigens and several functions such as antigen presenting cell activity, susceptibility to oxidant stress, and the susceptibility to HIV-1 and *mycobacterium tuberculosis* infection were examined.

Results: GM-Mφs and M-Mφs are distinct in their morphology, cell surface antigen expression, and functions examined. The phenotype of GM-Mφs closely resembles that of human Alveolar-Mφs (A-Mφs), indicating that CSF-induced human monocyte-derived Mφs are useful to clarify the molecular mechanism of heterogeneity of human Mφs, and GM-Mφs will become a model of human A-Mφs.

Key words: catalase, colony-stimulating factors, HIV-1, macrophages, *mycobacterium tuberculosis.*

INTRODUCTION

Macrophages (Mφs) have various functions beside phagocytosis such as bactericidal activity, antigen-presentation, tumor cytotoxicity, removal of aged or damaged cells, repair of injured tissue, bone resorption and special lipid metabolism. Mφs produce and secrete a large array of small- and macro-molecules that mediate the recruitment of hematopoietic or other cells, control cell growth, differentiation and function, influence vascular permeability in inflammatory sites and attack target microorganisms. Therefore, Mφs play a critical role in the host defense and the maintenance of homeostasis.

Correspondence: Kiyoko S. Akagawa, Department of Immunology, National Institute of Infectious Diseases, Toyama 1-23-1, Shinjuku-ku, Tokyo 162-8640, Japan. Email: akagawak@nih.go.jp

Mφs exist in practically every tissue in the body, but Mφs from different tissues exhibit a wide range of phenotypes with regard to their morphology, cell surface antigen expression and function, and are called by different names. Mφs originate from hematopoietic stem cells in bone marrow, they are predominantly derived from circulating blood monocytes (Mos),[1] which enter various tissues and differentiate into tissue specific Mφ populations[2] under the influence of the microenvironment. The mechanisms mediating the terminal differentiation and heterogeneity of Mφs, however, are not well known but are of fundamental significance.

Granulocyte-macrophage colony-stimulating factor (GM-CSF) and macrophage-CSF (M-CSF) are two hematopoietic growth factors that are both implicated in regulating production and function of cells of Mo/Mφ lineage.[3–5] From the studies of mice, it is clear that GM-CSF regulates the phenotype and functions of Alveolar-Mφs (A-Mφs) critical to surfactant homeostasis and host defense.[6–8] In contrast, it is clear that

M-CSF plays an important role in the development, proliferation and differentiation of osteoclasts and certain tissue Mϕ populations such as peritoneal Mϕs.[9] Therefore, Mos recruited to the sites where either CSF is dominant might differentiate into a divergent phenotype of Mϕs, such as A-Mϕs and peritoneal Mϕs. In agreement with these studies, the authors' recent studies in human Mos indicate that M-CSF and GM-CSF stimulate the generation of two phenotypically distinct types of Mϕs (M-Mϕs and GM-Mϕs), and the phenotype of GM-Mϕs resembles that of human A-Mϕs.

METHODS

Cytokines

Recombinant human (rh) GM-CSF (1×10^8 U/mg) and rhM-CSF (1×10^8 U/mg) were provided by Schering-Plough Japan (Osaka, Japan) and Morinaga Milk Industry Co. Ltd. (Tokyo, Japan), respectively.

Preparation of monocyte-derived macrophages

Mos were obtained from PBMC of normal healthy volunteers using a magnetic cell separation system (MACS: Miltenyi Biotec, Bergisch Gladbach, Germany) with anti-CD14 mAb-coated microbeads. $CD14^+$ Mos were cultured in RPMI 1640 medium (Nissui Seiyaku Co. Ltd, Tokyo, Japan) supplemented with 10% heat-inactivated fetal calf serum (FCS: Z. L. Bockneck Laboratories Inc., Ontario, Canada) in the presence of the following human recombinant cytokines at optimal concentrations: 5 ng/mL GM-CSF (Schering-Plough Japan, Osaka, Japan) or 50 ng/mL M-CSF (Morinaga Milk Industry Co. Ltd.) at 37°C under a humidified 5% CO_2 atmosphere for 7 days. During the culture, Mos differentiated to Mϕs. Human A-Mϕs were obtained from healthy volunteers (non-smokers without diseases) by the BAL method. All volunteers gave informed consent to the use of their A-Mϕs for part of this study.

Measurement of catalase activity

Intracellular and extracellular catalase activity was measured according to the method described by Aebi.[10]

HIV-1 infection and antisense treatment of Hck and C/EBPβ

Macrophage-tropic HIV-1 strains ($HIV\text{-}1_{BaL}$, $HIV\text{-}1_{JR\text{-}FL}$) were used. Phosphorothioate-modified antisense oligonucleotides for Hck (AS-Hck: 5′-TTCATCGACC CCATCCTGGC-3′) and C/EBPβ (AS-C/EBPβ: 5′-CAG GCGTTGCATGAACGCGG-3′), and their corresponding sense oligonucleotides (S-Hck: 5′-GCCAGGATG GGGTCGATGAA-3′ and S-C/EBPβ: 5′-CCGCGTTCAT GCAACGCCTG-3′), and their unrelated nonsense oligonucleotides (NS-Hck: 5′-CCATATTTCCCGCTCGC GTG-3′ and NS- C/EBPβ: 5′-CCAGAGAGGGCCCGTGT GGA-3′) were synthesized.

Mycobacterium tuberculosis (*mycobacterium tuberculosis*) infection and colony-forming unit assay

Mϕs were infected with single-cell suspension of *mycobacterium tuberculosis* H37Rv at Moi of 1–2. Infected Mϕs were cultured for 5–7 days in an antibiotics-free culture medium and the number of bacteria in the culture supernatant and within the cells were counted with a colony-forming unit (CFU) assay using Middlebrook 7H10 agar supplemented with OADC. For the determination of the number of intracellular bacteria, Mϕs were lysed by the addition of 1 mL of distilled water supplemented with 0.05% Tween 80.

T cell proliferation assay

PBMC (10^5 cells/well) with or without Mϕs were stimulated with 10 μg/mL PPD for 5 days in a 96-well microtiter plate at 37°C, and T cell proliferation was determined by the ^3H-thymidine incorporation assay.

Assay for IL-10 and γ-interferon activities

Culture supernatants were harvested from Mϕs and Mϕs plus PBMC stimulated with or without PPD for 24 h and 72 h for the assay of IL-10 and γ-interferon (IF), respectively. The levels of IFN-γ and IL-10 were determined by an ELISA (Endogen).

Statistical analysis

Statistical analysis was performed with the Student's *t*-test.

RESULTS

Monocyte-derived macrophages induced by M-CSF and GM-CSF are different in their morphology and cell surface antigen expression

When blood Mos were cultured in medium alone *in vitro*, Mos died, and CSF such as M-CSF or GM-CSF were necessary for their survival and differentiation into Mϕs.[11] Mϕs induced by M-CSF (M-Mϕs) had an elongated and spindle-like morphology, though some small and round cells remained, but Mϕs induced by GM-CSF (GM-Mϕs) were round and had a fried egg-like morphology. As shown in Figure 1, the expression of cell surface antigens were different between M-Mϕs and GM-Mϕs.[12–14] The phenotype of GM-Mϕs (fried egg-like shape and $c\text{-}fms^{low}$, $CD14^{low}$, $CD71^+$ and $710F^+$) closely resembled that of human A-Mϕs. In contrast, the morphology and the expression of cell surface antigens ($c\text{-}fms^{high}$, $CD14^{high}$) of M-Mϕs resembled that of human peritoneal Mϕs or influx Mϕs induced by inflammation.

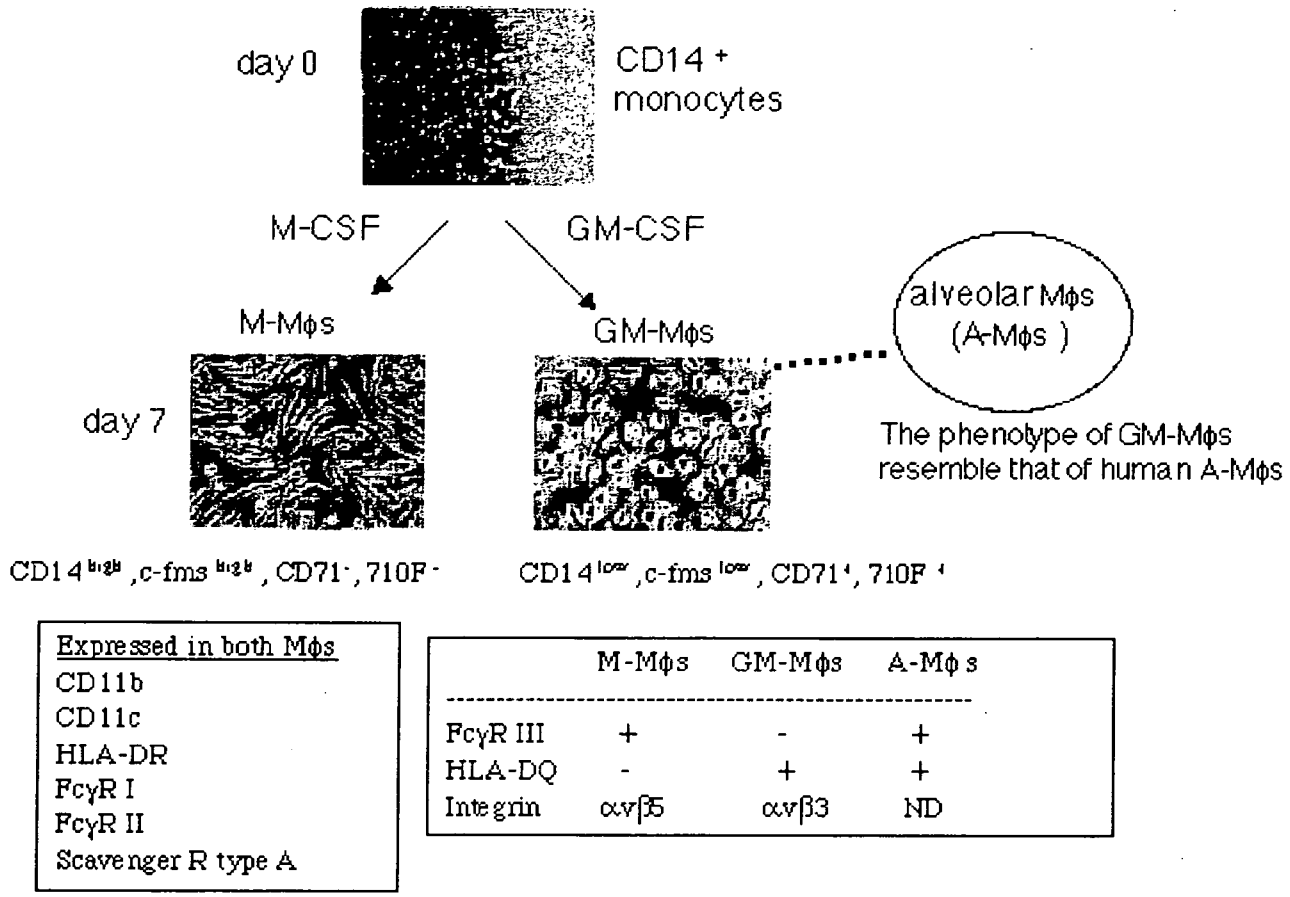

Figure 1 Effects of colony-stimulating factors on the differentiation of monocytes into macrophages.

Monocyte-derived macrophages induced by GM-CSF and M-CSF are different in their capacity for FcγR-mediated phagocytosis

Both M-Mϕs and GM-Mϕs ingested latex particles, but their capacity for FcγR-mediated phagocytosis was significantly different. More than 98% of M-Mϕs phagocytized sensitized erythrocytes (EA), whereas only about 30% of GM-Mϕs did.[13] Both types of Mϕ could form rosettes in a similar manner with EA. Therefore, the defect in GM-Mϕs may be located at the level of the signal transduction pathway need for ingestion after the binding of EA to FcγR.

Monocyte-derived macrophages induced by GM-CSF and alveolar macrophages but not monocyte-derived macrophages induced by M-CSF are resistant to H_2O_2 via their high basal and inducible levels of catalase activity

Mϕs produce and release reactive oxygen species (ROS), such as H_2O_2, O_2^-, and OH, in response to phagocytosis or stimulation with various agents through activation of a multicomponent NADPH oxidase. ROS are essential for the killing of a wide variety of microbes. In addition, ROS have been implicated in inflammation and tissue injury. M-Mϕs produced a large amount of H_2O_2 compared with GM-Mϕs in response to zymosan or heat-killed *Staphylococcus aureus*.[15] GM-Mϕs were highly resistant to H_2O_2, and expressed high levels of catalase activity. In contrast, M-Mϕs expressed low catalase activity, and were about 50-fold more sensitive to H_2O_2 than GM-Mϕs. The antioxidant state of A-Mϕs was at a similar level to that of GM-Mϕs by assessment of H_2O_2 sensitivity and catalase activity. About 1–10 mmol/L H_2O_2, similar to levels found on exhalation in cases of adult respiratory distress syndrome, did not induce cell death of either GM-Mϕs or A-Mϕs. GM-Mϕs and A-Mϕs but not M-Mϕs could induce catalase expression in both protein and mRNA levels when stimulated with H_2O_2 or zymosan. These findings indicate that GM-Mϕs and A-Mϕs but not M-Mϕs are strong scavengers of H_2O_2 via a high basal level of catalase activity and a marked ability of catalase induction.

Different susceptibility of monocyte-derived macrophages induced by M-CSF and GM-CSF to macrophage-tropic HIV-1

Recent studies indicate that human Mos/Mϕs are a primary target for initial HIV-1 infection and a

major reservoir for latent infection.[16,17] M-Mϕs had a great capacity to produce HIV-1, while GM-Mϕs inhibited HIV-1 replication.[18,19] Similar levels of viral DNA formation were observed in both types of Mϕ after HIV-1infection, indicating that the inhibition of HIV-1 replication in GM-Mϕs occurs at post-transcriptional and translational levels but not at the viral entry. M-Mϕs expressed a high level of Hck, which can bind HIV-1Nef and a large isoform of C/EBPβ, and HIV-1 infection increased the expression of Hck but not of C/EBPβ. GM-Mϕs expressed a high level of C/EBPβ and a low level of Hck, and HIV-1 infection drastically increased the expression of a short isoform of C/EBPβ, which acts as a dominant negative transcription factor, but decreased that of Hck. Treatment of M-Mϕs with antisense oligonucleotide for Hck not only suppressed the expression of Hck, but also stimulated the induction of the short isoform of C/EBPβ and inhibited viral replication. Treatment of GM-Mϕs with antisense oligonucleotide for C/EBPβ not only preferentially inhibited the expression of the small isoform of C/EBPβ, but also stimulated the induction of Hck and stimulated the virus production at a high rate. These results suggest that the CSF-induced and HIV-1-mediated distinct regulation of Hck and small isoform of C/EBPβ represent the heterogeneous susceptibility of tissue Mϕs to HIV-1 infection. The authors also found that A-Mϕs from healthy volunteers dominantly expressed a low level of Hck and small isoform of C/EBPβ and hardly stimulated HIV-1 replication, indicating GM-Mϕs resemble A-Mϕs in their susceptibility to HIV-1 infection.

Monocyte-derived macrophages induced by M-CSF but not GM-CSF can inhibit the growth of *Mycobacterium tuberculosis* and kill the bacteria

M. tuberculosis is a major human pathogen that resides in the host lung as a facultative intracellular pathogen and is found primarily in A-Mϕs. M-Mϕs inhibited the growth of *M. tuberculosis* H37Rv and killed the bacteria, while GM-Mϕs stimulated the growth. H_2O_2 and NO were not the effector molecules of M-Mϕs against *M. tuberculosis*, because addition of catalase or a NO synthesis inhibitor did not significantly change the bacterial killing activity of M-Mϕs, and the levels of NO produced by infected M-Mϕs and GM-Mϕs were very low and no significant difference was observed between them. When Mϕs were infected with *M. tuberculosis*, augmented expression of NRAMP1 (SLC11A1) and strong activation of p38MAPK, ERK1/2 and JNK were observed in M-Mϕs but not in GM-Mϕs. These results indicate that the difference in the activation of MAPK and the augmented expression of NRAMP1 may be related to the distinct susceptibility of M-Mϕs and GM-Mϕs to *M. tuberculosis*.

Monocyte-derived macrophages induced by M-CSF but not GM-CSF produce IL-10 and inhibit the γ-interferon production by T cells

M-Mϕs and GM-Mϕs are distinct in their suppressor activity. M-Mϕs and GM-Mϕs equally suppressed T cell proliferation in PBMC stimulated with PPD, but only M-Mϕs suppressed IFN-γ production by T cells in response to PPD.[20] M-Mϕs but not GM-Mϕs released a large amount of IL-10 in response to PPD, and the neutralizing antibody to IL-10 reversed the suppressor activities of M-Mϕs on IFN-γ production but not lymphocyte proliferation. Production of IFN-γ by lymphocytes was markedly inhibited by exogenous IL-10, while exogenous IL-10 was not as potent as M-Mϕs for suppressing lymphocyte proliferation. Therefore, the mechanism of M-Mϕ mediated T cell suppression for IFN-γ production is largely attributed to IL-10. A-Mϕs from rodents and humans selectively inhibit T-cell proliferation but permit cytokine secretion, such as interleukin-2 and IFN-γ.[21] In respect to the lacking of suppressor activity for IFN-γ production, but not for proliferation, by T cells, GM-Mϕs resemble A-Mϕs.

Down-regulation of IL-10 production by GM-Mϕs may be beneficial for host defense mechanisms against bacterial and viral infection to augment Th1 response. In contrast, M-Mϕs may play important roles in suppressing lymphocyte responses through potent immunosuppressive activity. Therefore, divergent macrophages play appropriate roles in different situations to maintain homeostasis in the host.

DISCUSSION

The present study shows that GM-CSF and M-CSF stimulate the differentiation of human monocytes into two phenotypically distinct types of macrophages *in vitro*. The phenotype and functions of GM-Mϕs resembles that of human A-Mϕs, indicating that GM-CSF plays an important role in the differentiation of human A-Mϕs. In the serial analysis of gene expression of monocytes, GM-Mϕs and M-Mϕs identified the specific gene expression in these cells along with the expression of large and overlapping sets of genes.[22,23] In addition, recent studies indicate the critical role of transcription factor PU.1 in GM-CSF-dependent terminal differentiation of mouse A-Mϕs.[24] However, the precise molecular mechanisms of the difference of GM-CSF- and M-CSF-dependent differentiation of Mϕs are not yet fully known. A model system using CSF-induced human Mo-derived M-Mϕs and GM-Mϕs may contribute the precise analysis of the molecular mechanisms.

ACKNOWLEDGEMENTS

This study was supported in part by grants from the Human Science Research Foundation and the Ministry of Health, Labour and Welfare of Japan.

REFERENCES

1 Kennedy DW, Abkowitz JL. Mature monocytic cells enter tissues and engraft. *Proc. Natl. Acad. Sci. USA* 1998; **95**: 14944–9.

2 Hume DA, Robinson AP, MacPherson GG, Gordon S. The mononuclear phagocyte system of the mouse defined by immunohistochemical localization of antigen F4/80: Relationship between macrophages, Langerhans cells, reticular cells, and dendritic cells in lymphoid and hematopoietic organs. *J. Exp. Med.* 1983; **158**: 1522–36.

3 Burdach S, Nishinakamura R, Dirksen U, Murray R. The physiologic role of interleukin-3, interleukin-5, granulocyte-macrophage colony-stimulating factor, and the beta c receptor system. *Curr. Opin. Hematol.* 1998; **5**: 177–80.

4 Motoyoshi K. Macrophage colony-stimulating factor. *Nippon Rinsho* 1999; **57**: 765–8 (in Japanese).

5 Motoyoshi K. Biological activities and clinical application of M-CSF. *Int. J. Hematol.* 1998; **67**: 109–22.

6 Akagawa KS, Kamoshita K, Tokunaga T. Effects of granulocyte-macrophage colony-stimulating factor and colony-stimulating factor-1 on the proliferation and differentiation of murine alveolar macrophages. *J. Immunol.* 1988; **141**: 3383–90.

7 Dranoff G, Crawford AD, Sadelain M *et al.* Involvement of granulocyte-macrophage colony-stimulating factor in pulmonary homeostasis. *Science* 1994; **264**: 713–16.

8 Robb L, Drinkwater CC, Metcalf D *et al.* Hematopoietic and lung abnormalities in mice with a null mutation of the common beta subunit of the receptors for granulocyte-macrophage colony-stimulating factor and interleukins 3 and 5. *Proc. Natl. Acad. Sci. USA* 1995; **92**: 9565–9.

9 Naito M, Umeda S, Takahashi K, Shultz LD. Macrophage differentiation and granulomatous inflammation in osteopetrotic mice (op/op) defective in the production of CSF-1. *Mol. Reprod. Dev.* 1997; **46**: 85–91.

10 Aebi H. Catalase *in vitro*. *Methods Enzymol.* 1984; **105**: 121–6.

11 Akagawa KS, Takasuka N, Nozaki Y *et al.* Generation of CD1+RelB+ dendritic cells and tartrate-resistant acid phosphatase-positive osteoclast-like multinucleated giant cells from human monocytes. *Blood* 1996; **88**: 4029–39.

12 Akagawa K. Differentiation and function of human monocytes. *Hum. Cell* 1994; **7**: 116–20 (in Japanese).

13 Akagawa KS. Generation of two phenotypically distinct types of macrophages, CD1+ dendritic cells and TRAP+ osteoclast-like multi-nucleated giant cells from human monocytes. *Nippon Ishinkin Gakkai Zasshi* 1997; **38**: 209–14.

14 Hashimoto SI, Komuro I, Yamada M, Akagawa KS. IL-10 inhibits granulocyte-macrophage colony-stimulating factor-dependent human monocyte survival at the early stage of the culture and inhibits the generation of macrophages. *J. Immunol.* 2001; **167**: 3619–25.

15 Komuro I, Keicho N, Iwamoto A, Akagawa KS. Human alveolar macrophages and granulocyte-macrophage colony-stimulating factor-induced monocyte-derived macrophages are resistant to H_2O_2 via their high basal and inducible levels of catalase activity. *J. Biol. Chem.* 2001; **276**: 24360–4.

16 Ghorpade A, Xia MQ, Hyman BT *et al.* Role of the beta-chemokine receptors CCR3 and CCR5 in human immunodeficiency virus type 1 infection of monocytes and microglia. *J. Virol.* 1998; **72**: 3351–61.

17 Lane BR, Markovitz DM, Woodford NL, Rochford R, Strieter RM, Coffey MJ. TNF-alpha inhibits HIV-1 replication in peripheral blood monocytes and alveolar macrophages by inducing the production of RANTES and decreasing C-C chemokine receptor 5 (CCR5) expression. *J. Immunol.* 1999; **163**: 3653–61.

18 Matsuda S, Akagawa K, Honda M, Yokota Y, Takebe Y, Takemori T. Suppression of HIV replication in human monocyte-derived macrophages induced by granulocyte/macrophage colony-stimulating factor. *AIDS Res. Hum. Retroviruses* 1995; **11**: 1031–8.

19 Komuro I, Yokota Y, Yasuda S, Iwamoto A, Akagawa KS. CSF-induced and HIV-1-mediated distinct regulation of Hck and C/EBPbeta represent a heterogeneous susceptibility of monocyte-derived macrophages to M-tropic HIV-1 infection. *J. Exp. Med.* 2003; **198**: 443–53.

20 Mochida-Nishimura K, Akagawa KS, Rich EA. Interleukin-10 contributes development of macrophage suppressor activities by macrophage colony-stimulating factor, but not by granulocyte-macrophage colony-stimulating factor. *Cell Immunol.* 2001; **214**: 81–8.

21 Upham JW, Strickland DH, Robinson BW, Holt PG. Selective inhibition of T cell proliferation but not expression of effector function by human alveolar macrophages. *Thorax* 1997; **52**: 786–95.

22 Hashimoto S, Suzuki T, Dong HY, Yamazaki N, Matsushima K. Serial analysis of gene expression in human monocytes and macrophages. *Blood* 1999; **94**: 837–44.

23 Hashimoto S, Nagai S, Sese J *et al.* Gene expression profile in human leukocytes. *Blood* 2003; **101**: 3509–13.

24 Shibata Y, Berclaz PY, Chroneos ZC, Yoshida M, Whitsett JA, Trapnell BC. GM-CSF regulates alveolar macrophage differentiation and innate immunity in the lung through PU.1. *Immunity* 2001; **15**: 557–67.

結核菌薬剤感受性検査のためのBACTEC MGIT 960 ASTの評価：外部精度管理菌株を用いた研究

[1]小林 郁夫 [1]阿部千代治 [2]御手洗 聡

要旨：〔目的〕迅速な結核菌薬剤感受性検査法であるBACTEC MGIT 960結核菌薬剤感受性検査用ミジットシリーズ（Mycobacterium Growth Indicator Tube Antimicrobial Susceptibility Testing: MGIT AST）の精度を調べた。〔材料と方法〕評価にはWHO/IUATLDが薬剤感受性検査の外部精度アセスメントに使用している菌株と結核菌H37Rvを用いた。MGIT ASTとMiddlebrook 7H10寒天培地による比率法（比率法）でイソニアジド（INH），リファンピシン（RFP），ストレプトマイシン（SM），エタンブトール（EB）に対する感受性を測定した。得られた結果はWHO/IUATLDのSupranational Reference Laboratory Network（SRLN）の結果と比較した。〔結果〕INHとRFPの検査では，SRLNの成績を標準としたときMGIT ASTの感度，特異性，一致率，再現性のいずれも100%であった。SMの検査について，MGIT ASTのSRLNの結果との一致率は97.9%，EBの検査は91.5%であり，主要4薬剤について90%以上の一致率を示した。〔結論〕今回の結果からMGIT ASTはWHO/IUATLDが目標として掲げた薬剤感受性検査の精度，すなわち検査の感度，特異性，再現性および一致率を満足させる迅速な検査であると考えられる。

キーワーズ：MGIT AST，薬剤感受性検査，結核菌，WHO/IUATLD

はじめに

薬剤感受性検査の結果は患者の治療のみならず薬剤耐性結核菌の出現にも影響を与えることから，検査の精度管理は重要である。薬剤感受性検査は抗酸菌の検査の中で最も精度管理の難しい検査である。世界保健機関（World Health Organization: WHO）と国際結核肺疾患予防連合（International Union Against Tuberculosis and Lung Disease: IUATLD）は世界的規模で薬剤耐性結核のサーベイランスを実施するにあたり，世界で20数カ所の研究所または大学の研究室をSupranational Reference Laboratory（SRL）に選び，薬剤感受性検査の精度管理研究をスタートさせた[1]。WHO/IUATLDのコーディネーターからSRLに薬剤耐性菌を含む結核菌を送付し，SRLのネットワーク（SRLN）で標準化し，それらの菌株をサーベイランス実施国の精度管理に用いている。わが国でも日本結核病学会抗酸菌検査法検討委員会が上記の菌株を用いて医療機関や検査センターを対象に薬剤感受性検査の外部精度アセスメントを実施しており[2)3)]，その結果手技の習熟や使用する方法による特性を把握することなど，改めて精度管理の重要性が明らかになった。

検査の所要日数の長短は患者の治療や管理に影響することから，時宜にかなった検査結果の報告は微生物検査室に課せられた重要な責務である。わが国で現在用いている小川培地による結核菌の薬剤感受性検査は結果を得るまでに約1カ月を要することから，より短時間で結果が得られる検査が望まれている。米国のCenters for Disease Control and Prevention（CDC）から出された検査の所要日数についての提案では，検体入手後結核菌の薬剤感受性検査の結果を30日以内に臨床医に報告することとしており[4)5)]，これは固形培地を用いた従来法で達成することは不可能である。液体培地を用いるBACTEC 460 TBやMGIT ASTシステムの迅速性と有用性に関する報告は数多くみられる[6)~12)]。米国やヨーロッパ諸国では液

[1]日本ベクトン・ディッキンソン株式会社ダイアグノスティックス事業部，[2]結核予防会結核研究所抗酸菌レファレンスセンター細菌検査科

連絡先：小林郁夫，日本ベクトン・ディッキンソン株式会社ダイアグノスティックス事業部，〒960-2152 福島県福島市土船字五反田1（E-mail: ikuo_kobayashi@bd.com）

(Received 19 Oct. 2005/Accepted 9 Nov. 2005)

体培地を用いる薬剤感受性検査が推奨されており，わが国でも今後普及していくものと思われる。

以前にわれわれは臨床分離株を用いMGIT ASTと小川法の成績を比較した結果を報告した[10]。今回WHO/IUATLDが薬剤感受性検査の外部精度アセスメントに使用している菌株を用い，MGIT ASTの精度を再評価したので報告する。

検査材料と方法

（1）菌株

WHO/IUATLDのコーディネーターから分与された結核菌50株と結核菌H37Rv（ATCC 27294）を評価に用いた。これらの結核菌はWHO/IUATLDのSRLNで標準化された菌株である。

（2）接種菌液の調製

被検菌を2%小川培地に接種後37℃で約4週間培養した。培地表面の集落を満遍なくかきとり5mLのMiddlebrook 7H9培地に懸濁後37℃で静置培養した。毎日1回撹拌し，培養液の濁度がMcFarland #0.5を超えるまで培養した。濁度計と滅菌蒸留水を用い，培養液からMcFarland #0.5濁度の菌液を調整した。

（3）MGIT AST

BACTEC MGIT 960結核菌薬剤感受性検査用ミジットシリーズの添付文書に従い，結核菌薬剤感受性用MGITチューブに専用サプリメントと薬剤を添加した。検査に用いた薬剤の濃度は，INH: 0.1 μg/mL，RFP: 1.0 μg/mL，SM: 1.0 μg/mL，EB: 5.0 μg/mLであった。McFarland #0.5に調整した菌液を滅菌蒸留水で5倍希釈し，薬剤添加MGITチューブへの接種菌液とした。コントロール用MGITチューブへの接種には，接種菌液を滅菌蒸留水でさらに100倍希釈したものを用いた。菌液を各MGITチューブに0.5mL接種後，直ちにBACTEC MGIT 960全自動抗酸菌培養装置（MGIT 960）で培養を開始した。MGIT ASTは，培養開始4日目より13日目までの間にコントロール用MGITチューブの菌発育を示す蛍光強度が一定値を越えた時点で薬剤添加MGITチューブの蛍光強度を測定し，個々の薬剤に対する被検菌の感受性を判定するシステムである。

（4）Middlebrook 7H10培地による比率法

National Committee for Clinical Laboratory Standards（現CLSI: Clinical and Laboratory Standards Institute）M24-Aに記載されている方法に従いMiddlebrook 7H10寒天培地を調製した[13]。検査に用いた薬剤の濃度は，INH: 0.2 μg/mL，RFP: 1.0 μg/mL，SM: 2.0 μg/mL，EB: 5.0 μg/mLであった。McFarland #0.5に調整した菌液を滅菌蒸留水で100倍希釈し，薬剤添加Middlebrook 7H10寒天培地への接種菌液とした。コントロール用Middlebrook 7H10寒天培地への接種には，接種菌液を滅菌蒸留水でさらに100倍希釈したものを用いた。菌液を各培地に塗布後5%CO_2条件下37℃で培養し，3週目に判定した。

（5）評価方法

MGIT ASTおよびMiddlebrook 7H10寒天培地による比率法（比率法）の結果について，WHO/IUATLDのSRLNの結果を標準として感度，特異性，一致率，耐性的中率（PV-R），感受性的中率（PV-S）を計算し評価した[1]。感度はSRLNの結果が耐性のものを正しく耐性と判定した割合，特異性はSRLNの結果が感受性のものを正しく感受性と判定した割合，一致率はSRLの結果がそれぞれの薬剤について耐性，もしくは感受性と判定したものを同様に判定した割合である。PV-Rは耐性と判定したとき，その判定が正解である確率，PV-Sは感受性と判定したときの正解率である。なお，今回評価に用いた菌株の中でSRLN内の一致率が70%以下の菌株はRFPの検査で6株，SMで3株，EBで3株あり，これらはそれぞれの薬剤についての精度計算から除外した。

MGIT ASTの再現性は，被検菌の中から無作為に選んだ6菌株を用い，MGIT ASTの4薬剤について1日3回，3日間繰り返し（1菌株，1薬剤につき計9回の検査）測定し，SRLNの結果との一致率で評価した。

結　果

（1）MGIT ASTの再現性試験

無作為に選んだ6株を用いMGIT ASTシステムの再現性を調べた。計212検査を行い，全体の一致率は95.3%であった（Table 1）。INHとRFPの試験の一致率は100%であったが，SMとEBの試験でSRLNの結果と一部異なる成績がみられた。特にEBの試験で一致率は90%以下であった。

（2）外部精度アセスメント株を用いたMGIT ASTシステムの評価

WHO/IUATLDのSRLNで精度アセスメントに使用している50株の臨床分離結核菌および結核菌標準株H37Rvを用いMGIT ASTの精度を評価した。同時にCLSIが標準法としているMiddlebrook 7H10寒天培地を用いる比率法で検査を行い比較した。

INH感受性検査では，MGIT ASTの結果はSRLNの結果とすべて一致した（Table 2）。感度，特異性，一致率，PV-R，PV-Sのいずれも100%であった（Table 3）。比率法の結果はMGIT ASTの成績と同様にSRLNの結果といずれも100%一致した。

使用した50株のうち，6株はRFPの感受性検査でSRLN内の一致率が70%以下であったためRFPの精度計算から除外し，44株の結果で評価した。RFP感受性検査ではINHの検査と同様にMGIT ASTの結果はSRLNの

Table 1 Reproducibility testing of the BACTEC MGIT 960 AST system

Drug	No. of results	No. of results agreeing with SRLN	Agreement (%)
Isoniazid	53	53	100
Rifampin	53	53	100
Streptomycin	53	49	92.5
Ethambutol	53	47	88.7
Total	212	202	95.3

Reproducibility was assessed with six strains of *M. tuberculosis* in triplicate from three separately prepared inocula (i.e., nine replicate per strain).

Table 2 Comparison of drug susceptibility test results

Drug	No. of isolates with the following results				
SRLN	R	R	R	S	S
MGIT	R	R	S	S	S
7H10	R	S	R	R	S
Isoniazid	32	0	0	0	18
Rifampin	18	0	0	0	26
Streptomycin	20	1	1	0	25
Ethambutol	15	0	4	2	26

SRLN: Referee results of the WHO/IUATLD Supranational Reference Laboratory Network
MGIT: BACTEC MGIT 960 AST system
7H10: Proportion method on Middlebrook 7H10 agar

Table 3 Comparison of the results with the BACTEC MGIT 960 AST system or proportion method on Middlebrook 7H10 agar with the results of the WHO SRL Network

	Sensitivity	Specificity	PV-R	PV-S	Agreement
BACTEC MGIT AST					
Isoniazid	100	100	100	100	100
Rifampin	100	100	100	100	100
Streptomycin	95.5	100	100	96.2	97.9
Ethambutol	78.9	100	100	87.5	91.5
Proportion method					
Isoniazid	100	100	100	100	100
Rifampin	100	100	100	100	100
Streptomycin	95.5	100	100	96.2	97.9
Ethambutol	100	92.9	90.5	100	95.7

Sensitivity: Ability to detect true resistance
Specificity: Ability to detect true susceptibility
PV-R: Predictive value for resistance
PV-S: Predictive value for susceptibility

結果と完全に一致した。感度，特異性，一致率，PV-R，PV-Sはすべて100%であった。比率法の結果もMGIT ASTとまったく同様であり，いずれも100%であった。

SMに対する感受性検査でSRLNの結果と不一致となった菌株はMGIT ASTと比率法でそれぞれ1株ずつ認められた。それらのうち1株はSRLNの結果が耐性をMGIT ASTで感受性として，別の株はSRLNで耐性と判定した株を比率法で感受性と判定していた（Table 2）。Table 3に示したようにSM検査におけるMGIT ASTおよび比率法のSRLNの結果との一致率は97.9%であった。

EBに対する感受性検査でSRLNの成績と不一致の結果を示した菌株はMGIT ASTで4株，比率法で2株認められた。MGIT ASTで不一致であった4株はいずれもSRLNで耐性と判定したものを感受性と判定していた。一方比率法で不一致の結果を示した2株ともSRLNで感受性と判定した菌株であり比率法で耐性と判定していた。MGIT ASTのSRLNの結果との一致率は91.5%，比率法の一致率は95.7%であった。

MGIT AST検査用チューブに菌接種後感受性の検査結果が得られるまでに要した日数は6日～13日の範囲であり，中央値は7日であった。一方比率法の所要日数は3週間であった。

考　察

WHO/IUATLDはINHとRFPの感受性検査の感度，特異性，再現性を95%以上に保つこと，SM，EBを加えた主要4薬剤について全体の一致率を90%以上に保つことを目標として掲げている。今回の実験で，MGIT ASTの結果はINHとRFPについてはすべての菌株でSRLNの結果と一致したことから感度，特異性，一致率，PV-R，PV-Sのすべてが100%であった（Table 3）。またINHおよびRFPの再現性試験の結果も100%であった。さらに，SMの一致率は97.9%，EBの一致率は91.5%であり，4薬剤の一致率は90%以上であった。これらの成績は，MGIT ASTがWHO/IUATLDの掲げた精度目標を満足させる検査であることを示している。なおWHO/IUATLDの検査精度アセスメントでは，SRLNの大多数が報告した結果をその菌株のゴールドスタンダードとして精度を計算しており[1]，SRLN内の一致率が70%以下の菌株はその結果をゴールドスタンダードとすることが不適当であると考え精度計算から除外している[15]。今回の研究では，SRLNの考えに従い一致率が70%以下の菌株を精度計算から除外した。

SRLNの成績と不一致の結果を示した株がMGIT ASTによるEBの検査で4株，SMの検査で1株みられた（Table 2）。これらの菌株の比率法による検査結果はSRLNと一致していた。EBの検査で不一致の結果を示した4株のうち3株はSRLN内でも80%以下（78.3%，78.9%，78.9%）の低い一致率であり，一部の株では検査法や検査条件により異なる結果が出ることが示された。残りの1株はSRLN内のEB検査で95.5%と高い一致率を示した株である。この株についてはMGIT ASTで検査を数回繰り返したが同じ結果であり，不一致の理由はわからない。SMの検査で不一致の結果を示した1株は，SRLN内での一致率は94.7%と高く，この株についても検査を繰り返したが同じ結果であり不一致の理由は不明である。

1994年からSRLN内で年1回薬剤感受性検査の精度試験を実施している。INHとRFPの検査精度は試験開始以来比較的良好であったが，SMとEBについては開始初期にはSRLN内の一致率が低かった[1][14][15]。特にEBは再現性を得ることが難しい薬剤であると考えられている[7]~[10][16][17]。Robertsらは Middlebrook 7H10寒天培地を用いる比率法をゴールドスタンダードとして比較したときBACTEC 460 TBによるEB検査の感度は66%を超えなかったと報告している[18]。今回のMGIT ASTによるEB検査の感度は78.9%であり，他の3薬剤についての検査の感度と比べ明らかに低い値であった。一方，Middlebrook 7H10寒天培地による比率法の感度は100%であった。EBの検査に用いている薬剤の濃度はMGIT ASTもMiddlebrook 7H10による比率法も同じ5 μg/mLであり，MGIT ASTの比較的低い感度は検査に用いた薬剤の濃度とは関係なく検査法の違いに起因しているものと考えられる。EBの検査で不一致の株はすべてSRLNで耐性と判定した株をMGIT ASTで感受性と判定しており，MGIT ASTでは感受性に判定される傾向がみられた。

MGIT ASTは迅速に結果が得られる検査として知られている[7]~[12]。今回の実験で菌接種後測定が終了するまでの所要日数は6日～13日の範囲（中央値：7日）であり，高い迅速性が再確認された。検査材料の入手後MGITによる結核菌の検出までに要する平均日数は約2週間である[19]~[23]。液体培養で陽性を示した培養液の少量を結核菌群特異抗原であるMPB64を検出するキャピリアTBのサンプルウエルに添加し15分静置することで迅速に結核菌群を鑑別できる[24][25]。同定結果が結核菌群であれば陽性MGITチューブの培養液から直接MGIT ASTで薬剤感受性を検査できる。このように，一連の検査に液体培地に基づくMGITシステムを用いることにより，分離，同定，薬剤感受性のすべての検査結果を30日以内に担当医に報告することとする目標を達成することが可能である。

結核の診断をより早期に行うことは患者の治療のみならず，感染拡大の防止，予防，ひいてはわが国の結核罹患率の減少に大きく影響する。迅速かつ精度の高い方法を組み合わせて早期の診断，治療に有用な検査情報を提供することは微生物検査室の大きな責務である。現在入院期間の短縮が求められており，迅速に薬剤感受性を測定できるMGIT ASTシステムは，今後の結核の診断治療に非常に有用であると考えられる。

謝　辞

結核菌株を分与いただいたWHO/IUATLDのコーディネーターであるLaszlo博士（WHO Collaborating Centre for Tuberculosis Bacteriology, Ottawa）およびPortaelsとvan Deunの両博士（Mycobacteriology Unit, Institute of Tropical Medicine, Antwerpen）に深謝します。また本研究は日本ベクトン・ディッキンソン株式会社 高橋洋氏の協力のもとに行われた。なお本論文の趣旨は第80回日本結核病学会総会（2005年5月12日，大宮）で発表した。

文　献

1）WHO/IUATLD Global Project on Anti-Tuberculosis Drug Resistance Surveillance: Anti-tuberculosis drug resistance in the world. WHO/TB 97.229. WHO, Geneva, Switzerland, 1998.

2) 日本結核病学会抗酸菌検査法検討委員会：抗酸菌検査の精度管理 (3) ―検査センターを対象とした結核菌薬剤感受性試験の外部精度アセスメント．結核．2005；80：47-48.
3) 御手洗聡：検査センターを対象とした結核菌薬剤感受性試験外部精度アセスメント．結核．2005；80：349-358.
4) Tenover FC, Crawford JT, Huebner RE, et al.: The resurgence of tuberculosis: is your laboratory ready? J Clin Microbiol. 1993; 31: 767-770.
5) CDC: National plan for reliable tuberculosis laboratory service using a system approach: recommendations from CDC and the Association of Public Heals Laboratories Task Force on tuberculosis laboratory service. Morbid Mortal Weekly Rep. 2005; 54 (RR-6): 1-12.
6) 鈴木克洋，露口一成，松本久子，他：Mycobacteria Growth Indicator Tube (MGIT) による結核菌迅速薬剤感受性検査．結核．1997；72：187-192.
7) Bemer P, Palicova F, Rüsch-Gerdes S, et al.: Multicenter evaluation of fully automated BACTEC Mycobacteria Growth Indicator Tube 960 system for susceptibility testing of *Mycobacterium tuberculosis*. J Clin Microbiol. 2002; 40: 150-154.
8) Tortoli E, Benedetti M, Fontanelli A, et al.: Evaluation of automated BACTEC MGIT 960 system for testing susceptibility of *Mycobacterium tuberculosis* to four major antituberculosis drugs: comparison with the radiometric BACTEC 460 TB method and the agar plate method of proportion. J Clin Microbiol. 2002; 40: 607-610.
9) Kontos F, Maniati M, Costopoulos C, et al.: Evaluation of the fully automated BACTEC MGIT 960 system for the susceptibility testing of *Mycobacterium tuberculosis* to first-line drugs: a multicenter study. J Microbiol Methods. 2004; 56: 291-294.
10) 阿部千代治，青野昭男，平野和重：BACTEC MGIT 960 システムによる結核菌の迅速薬剤感受性試験：固形培地を用いる比率法との比較．結核．2001；76：657-662.
11) 富田元久，竹野　華，鈴木克洋，他：バクテック MGIT 960による薬剤感受性検査における接種菌量の検討と検査の再現性．結核．2004；79：625-630.
12) 古畑由紀江，菊地勇治，田澤庸子，他：BACTEC MGIT™ 960結核菌薬剤感受性検査用ミジットシリーズの基礎的検討．JARMAM．2004；15：7-13.
13) NCCLS: Susceptibility testing of *Mycobacteria*, *Nocardia*, and other aerobic *Actinomycetes*; Approved Standard. NCCLS document M24-A, 2003.
14) WHO/IUATLD Global Project on Anti-Tuberculosis Drug Resistance Surveillance: Anti-tuberculosis drug resistance in the world. Report No.2. Prevalence and trend. WHO/CDS/TB 2000. 278. WHO, Geneva, Switzerland, 2000.
15) WHO/IUATLD Global Project on Anti-Tuberculosis Drug Resistance Surveillance: Anti-tuberculosis drug resistance in the world. Report No.3. WHO/HTM/TB/2004. 343. WHO, Geneva, Switzerland, 2004.
16) Bergmann JS, Woods GL: Reliability of Mycobacteria Growth Indicator Tube for testing susceptibility of *Mycobacterium tuberculosis* to ethambutol and streptomycin. J Clin Microbiol. 1997; 35: 3325-3327.
17) Siddiqi SH, Libonati JP, Middlebrook G: Evaluation of a rapid radiometric method for drug susceptibility testing of *Mycobacterium tuberculosis*. J Clin Microbiol. 1981; 13: 908-912.
18) Roberts GD, Goodman NL, Heifets L, et al.: Evaluation of the BACTEC radiometric method for recovery of mycobacteria and drug susceptibility testing of *Mycobacaterium tuberculosis* from acid-fast smear positive specimens. J Clin Microbiol. 1983; 18: 689-696.
19) 阿部千代治：酸素反応性蛍光センサーを用いた新しい抗酸菌迅速培養システムの検討．感染症誌．1996；70：360-365.
20) 斉藤　肇，螺良英郎，山中正彰，他：MGIT (Mycobacteria Growth Indicator Tube) の評価に関する10施設での共同研究．臨床と微生物．1997；24：897-903.
21) 三浦隆雄，長谷川直樹，鈴木紀久雄，他：MGIT (Mycobacteria Growth Indicator Tube) 抗酸菌検査システムの検出率と迅速性の評価．日本臨床微生物学雑誌．2000；10：125-130.
22) Hanna BA, Ebrahimzadeh A, Elliott LB, et al.: Multicenter evaluation of the BACTEC MGIT 960 system for recovery of mycobacteria. J Clin Microbiol. 1999; 37: 748-752.
23) 青野昭男：最近の抗酸菌検査：培養検査 MGIT．臨床と微生物．2001；28：253-261.
24) Abe C, Hirano K, Tomiyama T: Simple and rapid identification of the *Mycobacterium tuberculosis* complex by immunochromatographic assay using anti-MPB64 monoclonal antibodies. J Clin Microbiol. 1999; 37: 3693-3697.
25) Hasegawa N, Miura T, Ishii K, et al.: New simple and rapid test for culture confirmation of *Mycobacterium tuberculosis* complex: a multicenter study. J Clin Microbiol. 2002; 40: 908-912.

Original Article

BACTEC MGIT 960 SYSTEM FOR DRUG SUSCEPTIBILITY TESTING OF *MYCOBACTERIUM TUBERCULOSIS*: A STUDY USING EXTERNAL QUALITY ASSESSMENT STRAINS

[1]Ikuo KOBAYASHI, [1]Chiyoji ABE, and [2]Satoshi MITARAI

Abstract [Objective] To evaluate the performance of the BACTEC MGIT 960 system for drug susceptibility testing (MGIT AST) of *Mycobacterium tuberculosis* to isoniazid, rifampin, streptomycin and ethambutol.

[Design] Fifty external quality assessment strains of *M. tuberculosis* provided by the Coordinating Centers of WHO/IUATLD were tested by BACTEC MGIT 960 system, and the results were compared with the referee results of the WHO/IUATLD Supranational Reference Laboratory Network (SRLN).

[Results and conclusion] Overall concordance rates of the results obtained by MGIT AST and the referee results of the SRLN were 97.3% for four first-line drugs. Agreement rates were particularly high for isoniazid, rifampin, and streptomycin (agreement rate of over 97%), but somewhat lower for ethambutol, which relates to a lower sensitivity of MGIT AST. Turnaround times from inoculation to drug susceptibility results ranged from 6 to 13 days for the MGIT AST system with a median time of 7 days; this contrasted with three weeks for the proportion method using Middlebrook 7H10 agar, indicating that MGIT AST system has the potential to consistently meet with the turnaround time guidelines suggested by the Centers for Disease Control and Prevention of the United States. These results demonstrate that the fully automated BACTEC MGIT 960 AST system is useful for the rapid diagnosis of drug resistant tuberculosis.

Key words: MGIT AST, Susceptibility test, *Mycobacterium tuberculosis*, WHO/IUATLD

[1]Fukushima Laboratory, Nippon Becton Dickinson Company, Ltd. Japan, [2]Bacteriology Division, Mycobacterium Reference Center, Research Institute of Tuberculosis, Japan Anti-Tuberculosis Association

Correspondence to: Ikuo Kobayashi, Nippon Becton Dickinson Company, Ltd., 1 Gotanda, Tsuchifune, Fukushima-shi, Fukushima 960–2152 Japan.
(E-mail: ikuo_kobayashi@bd.com)

Respiratory Medicine (2005) 99, 1188–1190

ELSEVIER

respiratoryMEDICINE

CASE REPORT

Incipient stage of pulmonary Langerhans-cell histiocytosis complicated with pulmonary tuberculosis was examined by high-resolution computed tomography

Toru Arai[a], Yoshikazu Inoue[a,*], Satoru Yamamoto[a], Masanori Akira[a], Hiroyo Uesugi[b], Seiji Hayashi[a], Mitsunori Sakatani[a]

[a]*National Hospital Organization, Kinki-chuo Chest Medical Center, 1180 Nagasone-cho, Sakai City, Osaka 591-8555, Japan*
[b]*Tondabayashi Hospital, Tondabayashi, 1-3-36 Koyo-dai, Tondabayashi City, Osaka 584-0082, Japan*

Received 12 November 2004

KEYWORDS
Pulmonary Langerhans-cell histiocytosis;
High-resolution computed tomography;
Tuberculosis

Summary A 29-year-old man with a smoking history of 20 pack years was diagnosed with tuberculosis because *Mycobacterium tuberculosis* was detected in his gastric juice. His chest radiograph showed multiple nodular opacities on left upper lobe. He was treated with anti-tuberculosis drugs in our hospital. Six months after the therapy, he began to complain of dry cough and shortness of breath on exertion. Chest radiograph showed reticular opacities in both upper and middle lung fields. Multiple thick- and thin-walled bizarre-shaped cysts and ill-defined centrilobular opacities were seen mainly in upper and mid-lungs on high-resolution computed tomography (HRCT). He was diagnosed with pulmonary Langerhans-cell histiocytosis (PLCH) by transbronchial lung biopsy specimens from right upper lobe. HRCT findings before the treatment of tuberculosis were retrospectively examined. Several small thin-walled centrilobular cysts were scattered in the right upper and middle lung fields without apparent nodular lesions. We must consider the possibility of PLCH when these findings are detected on HRCT.

Introduction

Pulmonary Langerhans-cell histiocytosis (PLCH), previously referred to as pulmonary histiocytosis X or eosinophilic granuloma, is a disease of unknown etiology and pathologically characterized by

*Corresponding author. Tel.: +81 72 252 3021.
E-mail address: giichi@kch.hosp.go.jp (Y. Inoue).

0954-6111/$ - see front matter © 2005 Elsevier Ltd. All rights reserved.
doi:10.1016/j.rmed.2005.02.017

granulomas containing a large number of Langerhans cells localized in the lungs.[1] Although progression of the disease has been examined by high-resolution computed tomography (HRCT), the incipient stage of the disease is hard to examine because it insidiously progresses and patients with PLCH are asymptomatic up to 25%.[1] We could examine HRCT findings in a very early stage in this case.

Case report

A 29-year-old man with a smoking history of 20 pack years visited our hospital because of general fatigue. His chest radiograph showed multiple nodular opacities in the left upper lung field. By HRCT examination (Fig. 1a), large nodular lesions were surrounded with multiple small centrilobular nodules occurring in clusters and appearance of tree-in-bud. *Mycobacterium tuberculosis* was detected by culturing his gastric juice, and he was diagnosed with pulmonary tuberculosis. Administration of anti-tuberculosis drugs improved his general fatigue and nodular lesions on the chest radiograph decreased. Six month after the therapy, he began to complain of dry cough and shortness of breath on exertion. He visited our hospital again, because of the worsening of symptoms and occurrence of weight loss.

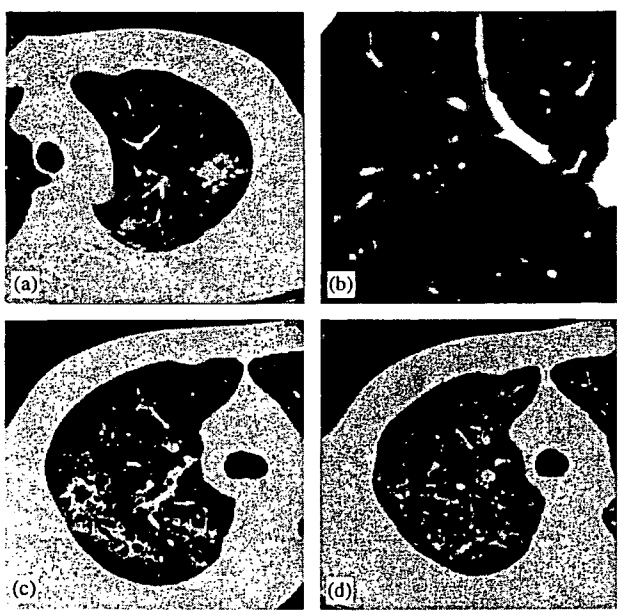

Figure 1 Radiological findings before treatment of tuberculosis (a and b) and after the onset of pulmonary Langerhans-cell histiocytosis (PLCH) (c and d). Before treatment of tuberculosis, high-resolution computed tomography (HRCT) of the left upper lobe showed large nodular lesions surrounded by multiple small centrilobular nodules occurring in clusters and appearance of tree-in-bud (a). Several small thin-walled centrilobular cysts were scattered in the right upper and middle lung field, although apparent nodular lesions suggesting PLCH were not detected (b). After the onset of PLCH, multiple thick- and thin-walled cysts and ill-defined centrilobular opacities were seen mainly in the upper and mid-lungs on HRCT (c). Thickness of the cysts was lessened and apparent centrilobular nodules decreased on HRCT after the cessation of smoking (d).

The chest radiograph on admission showed reticular opacities in both the upper and middle lung fields and the costophrenic angles were spared. Multiple thick- and thin-walled cysts and ill-defined centrilobular opacities were seen mainly in the upper and mid-lungs on HRCT (Fig. 1c). Some cysts showed bizarre shapes and branching appearance. The intervening lung parenchyma appears normal and without evidence of fibrosis or septal thickening. The well-defined nodular lesion supposed to be old tuberculosis was detected in the left upper lobe.

Cryptococcus antigen was not detected in his serum. Pathogenic organisms, including *Pneumocystis carinii*, or malignant cells were not detected in bronchoalveolar lavage (BAL) fluid performed in right B[5]. Transbronchial lung biopsy specimens from the right upper lobe showed bronchiolocentric nodular lesions, including proliferation of Langerhans cells with delicate and folded nuclei, and scattered eosinophils. He was diagnosed with PLCH.

HRCT findings before the treatment of tuberculosis were retrospectively examined. Although apparent nodular lesions suggesting PLCH were not detected, several small thin-walled centrilobular cysts were scattered in the right upper and middle lung field (Fig. 1b). These findings were suggested to arise from PLCH. We instructed him to abstain from smoking because PLCH is associated with smoking. Two months after that his shortness of breath and dry cough almost completely disappeared and thickness of the cysts was lessened and apparent centrilobular nodules decreased on HRCT (Fig. 1d).

Discussion

PLCH has been extensively investigated with HRCT.[2–4] Cysts and nodules are present in 80% and 50–80% of patients, respectively,[5] and the combination of nodules along with cysts predominantly in the upper and middle lung fields is a typical finding of PLCH.[1,5] The early stage of PLCH is characterized by ill-defined nodules, smaller than 5 mm and

distributed in a centrilobular pattern. These nodules are supposed to change into cavitated nodules and thick- and thin-walled cysts progressively.[1,5,6] Advanced diseases show substantial architectural distortion due to various-sized cysts with a few nodules. Thus, the HRCT findings of this case, in which small thin-walled cysts were present without nodular lesions in the upper lung fields, are not common for the incipient stage of PLCH.

The mechanism of cyst formation is explained by cavitation within a nodule resulting from granulomatous destruction, ball-valve effect in partially obstructed bronchioles by granuloma and traction bronchiectasis caused by interstitial fibrosis.[5] Apparent nodules were not detected before the treatment of tuberculosis in this case. Serial sections of open lung biopsies from patients of PLCH demonstrated granulomatous lesions are bronchiolocentric distribution.[7] Hence, we suppose that granulomas formed in the bronchiolar wall caused bronchiolectasis of the peripheral portion through the check-valve mechanism and this is the very early stage of PLCH.

Soler et al.[8] reported that radiological findings examined by HRCT suggest histological activity of PLCH. He demonstrated that densities of nodular lesions and thin-walled cysts on HRCT are correlated with densities of granulomas and cavitary lesions on histological specimens, respectively. But granulomas were detected in 2 out of 6 cases without nodular lesions on HRCT. Thus, no evidence of nodular lesions on HRCT cannot exclude the presence of active granulomatous lesions. We might be able to find granulomas by transbronchial lung biopsy at the time of an initial CT scan.

The majority of patients with selective pulmonary involvement of PLCH are heavy smokers and numbers of Langerhans cells of BAL increased in smokers.[9] Radiological predominance of PLCH lesions in the upper and mid-lung zones and pathological bronchiolocentric distribution of these[7] are common to other diseases associated with smoking and inhaled particles. Smoking cessation sometimes improves radiological findings and clinical symptoms of PLCH.[10] Thus, smoking is supposed to be associated with the disease and the clinical course of our case is consistent with the hypothesis.

Early diagnosis is important because no current treatment modality other than cessation of smoking is present for PLCH. Small centrilobular thin-walled cysts without nodules may be the very early stage of PLCH. Thus, we must consider the possibility of PLCH and carefully follow radiological changes, when only cystic lesions are found in HRCT.

Reference

1. Vassallo R, Ryu JH, Colby TV, et al. Pulmonary Langerhans-cell histiocytosis. *N Engl J Med* 2000;342:1969–78.
2. Moore ADA, Godwin JD, Muller NL, et al. Pulmonary histiocytosis X: comparison of radiographic and CT findings. *Radiology* 1989;172:249–54.
3. Schonfeld N, Frank W, Wenig S, et al. Clinical and radiologic features, lung function and therapeutic results in histiocytosis X. *Respiration* 1993;60:38–44.
4. Kulweic EL, Lynch DA, Aguayo SM, et al. Imaging of pulmonary histiocytosis X. *Radiographics* 1992;12: 515–26.
5. Sundar KM, Gosselin MV, Chung HL, et al. Pulmonary langerhans cell histiocytosis. Emerging concepts in pathobiology, radiology, and clinical evolution of disease. *Chest* 2003;123:1673–83.
6. Brauner MW, Grenier P, Mouelhi MM, et al. Pulmonary histiocytosis X: evaluation with high resolution CT. *Radiology* 1989;172:255–8.
7. Kambouchner M, Basset F, Marchal J, et al. Three-dimensional characterization of pathologic lesions in pulmonary langerhans cell histiocytosis. *Am J Respir Crit Care Med* 2002;166:1483–90.
8. Soler P, Bergeron A, Kambouchner M, et al. Tool to predict the histopathological activity of pulmonary langerhans cell histiocytosis. *Am J Respir Crit Care Med* 2000;162:264–70.
9. Soler P, Moreau A, Basset F, et al. Cigarette smoking-induced changes in the number and differentiated state of pulmonary dendritic cells/Langerhans cells. *Am Rev Respir Dis* 1989;139:1112–7.
10. Von Essen S, West W, Sitorius M, et al. Complete resolution of roentogenographic changes in a patient with pulmonary histiocytosis X. *Chest* 1990;142:1216–8.

JOURNAL OF CLINICAL MICROBIOLOGY, Nov. 2005, p. 5435–5439 Vol. 43, No. 11
0095-1137/05/$08.00+0 doi:10.1128/JCM.43.11.5435–5439.2005

Rapid Detection of *Mycobacterium tuberculosis* in Respiratory Samples by Transcription-Reverse Transcription Concerted Reaction with an Automated System

Shunji Takakura,[1]* Shigeo Tsuchiya,[2] Yuichi Isawa,[2] Kiyoshi Yasukawa,[2]† Toshinori Hayashi,[2] Motohisa Tomita,[3] Katsuhiro Suzuki,[3] Tatsuro Hasegawa,[4] Takanori Tagami,[4] Atsuyuki Kurashima,[4] and Satoshi Ichiyama[1]

Department of Clinical Laboratory Medicine, Kyoto University Graduate School of Medicine, 54 Shogoin-Kawaharacho, Sakyo-ku, Kyoto 6068507, Japan[1]; Scientific Instruments Division, Tosoh Corporation, 2743-1 Hayakawa, Ayase, Kanagawa 2521123, Japan[2]; Clinical Research Center, Kinki-chuo Chest Medical Center, 1180 Nagasone-cho, Sakai, Osaka 5918555, Japan[3]; and National Tokyo Hospital, 3-1-1 Takeoka, Kiyoshe-shi, Tokyo 2048585, Japan[4]

Received 6 June 2005/Returned for modification 28 June 2005/Accepted 10 August 2005

The aim of this study was to evaluate the performance of the transcription-reverse transcription concerted (TRC) method for the detection of *Mycobacterium tuberculosis* complex (MTC) 16S rRNA in clinical respiratory samples for the diagnosis of pulmonary tuberculosis. TRC is a novel method that enables the rapid and the completely homogeneous real-time monitoring of isothermal sequence RNA amplification without any post-amplification procedure. The detection limit of the TRC method for MTC was one organism per 100 μl of sputum. The specificity of the method was confirmed by the absence of positive signals for sputum containing 10^6 *M. avium* or *M. kansasii* organisms per 100 μl. A total of 201 respiratory samples from patients diagnosed with or suspected of having tuberculosis were tested. Of the 72 MTC culture-positive samples, the TRC method was positive for 52 (sensitivity, 72.2%), whereas the Roche COBAS AMPLICOR PCR was positive for 58 (sensitivity, 80.6%). Both the TRC method and the COBAS AMPLICOR PCR showed no positive identification for any of the 129 culture-negative samples. The percent agreement between the two methods was 95% (191 of 201 samples). The high sensitivity and specificity together with shorter detection time (within 1 h) of the TRC method allow it to be proposed as a useful method for the rapid detection of MTC in respiratory samples.

The rapid detection and identification of *Mycobacterium tuberculosis* complex (MTC) in respiratory samples are extremely important for optimal diagnosis and effective treatment, as well as for prevention and control of tuberculosis transmission. Various molecular tests based on amplification and detection techniques have been devised for the detection of MTC in clinical samples (2, 14), such as the PCR-based COBAS AMPLICOR Mycobacterium system (Roche Diagnostics, Basel, Switzerland) (4–7), the transcription-mediated amplification-based Gen-Probe Amplified Mycobacterium Tuberculosis Direct Test system (Gen-Probe Inc., San Diego, CA) (5, 15, 16), the strand displacement amplification-based BDProbeTec ET system (Becton Dickinson, Franklin Lakes, NJ) (6, 8), and the ligase chain reaction-based Abbott LCx Mycobacterium tuberculosis assay system (Abbott Laboratories, North Chicago, IL) (1). While they are much more rapid than any culture-based method, these systems still require several hours to get results and involve some complicated procedures (14). Therefore, a faster molecular test with greater ease of manipulation as well as high sensitivity and specificity is desirable.

* Corresponding author. Mailing address: Department of Clinical Laboratory Medicine, Kyoto University Graduate School of Medicine, 54 Shogoin-Kawaharacho, Sakyo-ku, Kyoto 6068507, Japan. Phone: 81-75-751-3503. Fax: 81-75-751-3233. E-mail: stakakr@kuhp.kyoto-u.ac.jp.

† Present address: Department of Food Biology, Kyoto University Graduate School of Agricultural Science, Oiwake-cho, Kitashirakawa, Sakyo-ku, Kyoto 6068502, Japan.

Recently, we have reported on a novel method designated the transcription-reverse transcription concerted (TRC) method (9). This method, a schematic of which is shown in Fig. 1, is based on isothermal RNA amplification at 43°C with transcriptase and reverse transcriptase in the presence of the intercalation activating fluorescence (INAF) probe (10). Measurement of the fluorescence intensity of the reaction mixture with a dedicated multicolor detector enables completely homogeneous real-time monitoring of the amplification of specific RNA, while it requires only 30 min for simultaneous amplification and detection. We have used the TRC method to establish a system for the detection of specific mRNA transcripts: *tdh* and *trh* of *Vibrio parahaemolyticus* (13), *mecA* of methicillin-resistant *Staphylococcus aureus* (11), and *pab* of *M. tuberculosis* (9, 19).

This report concerns the establishment and evaluation of the TRC method-based targeting of MTC 16S rRNA (hereinafter abbreviated the "TRC method") for the direct detection of MTC in clinical respiratory samples. rRNA was chosen as the target to enable highly selective and sensitive detection because of its multicopy nature in a single cell. The sensitivity and specificity of the TRC method were compared with those of the COBAS AMPLICOR PCR for the direct detection of MTC in sputum samples.

MATERIALS AND METHODS

Preparation of standard RNAs for calibration. Standard RNA containing the target region for TRC amplification was prepared by the in vitro transcription of the SP6 promoter-bearing double-stranded DNA as the template for SP6 RNA

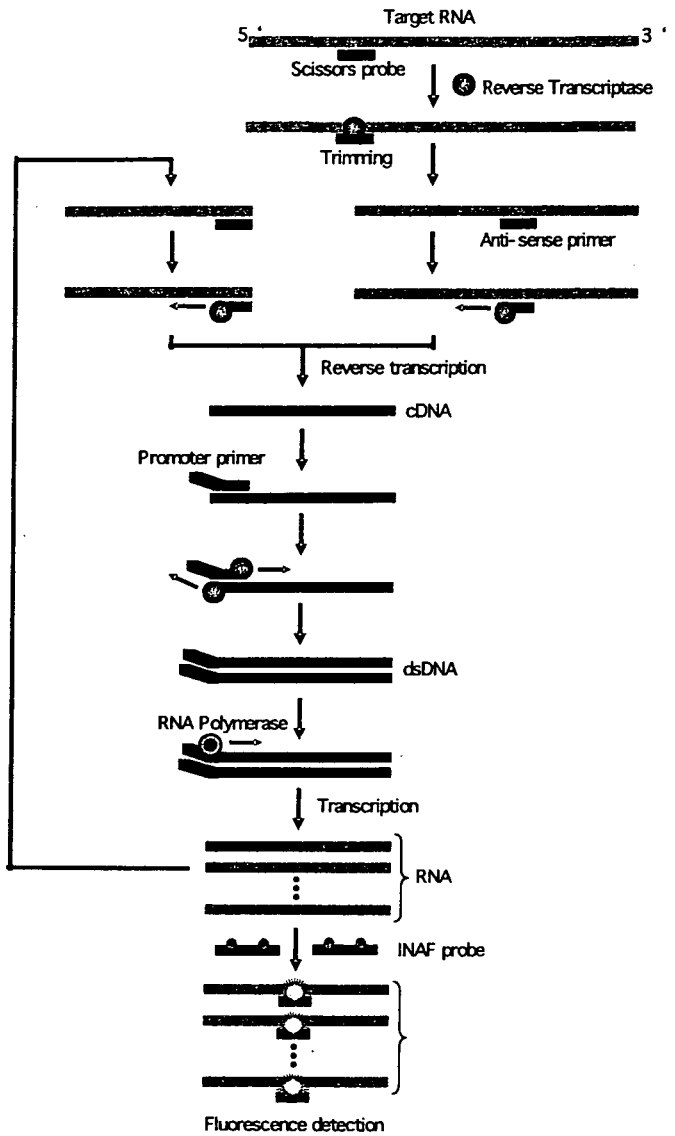

FIG. 1. Schematic description of the elementary steps of the TRC method. The progress of the reaction is monitored by measuring the fluorescence intensity of the reaction mixture. dsRNA, double-stranded RNA.

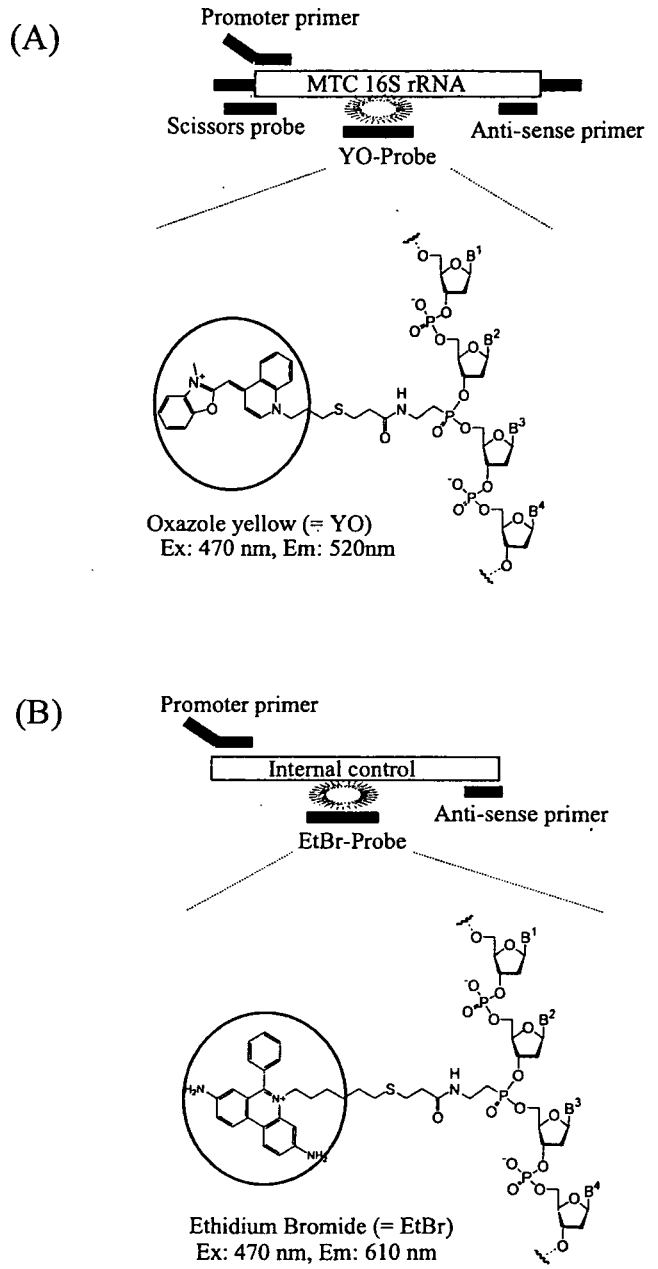

FIG. 2. Primers and probes used in the TRC method designed for amplification and detection of MTC 16S rRNA (A) and internal control (B). Ex, excitation wavelength; Em, emission wavelength.

polymerase. The DNA templates were synthesized from the total DNA extracted from the *Mycobacterium bovis* BCG strain (TOKYO 172; purchased from the National Institute of Infectious Diseases, Tokyo, Japan) by means of PCR (30 cycles of 95°C for 30 s, 55°C for 30 s, and 72°C for 3 min) with a pair of synthetic oligonucleotide primers, 5'-CGG TAC CCA TTT AGG TGA CAC TAT AGA ATA CAA GTT TTG TTT GGA GAG TTT GAT CC-3' and 5'-CGG TAC CCC TAC AGA CAA GAA CCC CTC A-3'. The long primer has the SP6 RNA polymerase-binding sequence at its 5' end (underlined) to provide the preferred transcription initiation site.

The amplified gene sequence was cloned into the EcoRI site of pUC19. The plasmid DNAs were then digested with EcoRI to yield linear DNAs containing the SP6 promoter, followed by in vitro transcription in a reaction mixture composed of 40 mM Tris-HCl (pH 7.5), 6 mM $MgCl_2$, 2 mM spermidine, 10 mM dithiothreitol, 0.5 mM nucleoside triphosphates, 0.1 mg/ml of bovine serum albumin, 1 U/ml of RNase inhibitor, 2.5 U/ml of SP6 RNA polymerase (TaKaRa Bio, Otsu, Shiga, Japan), and 0.025 mg/ml of template DNA. The resultant RNAs were purified by gel filtration with Chromaspin-100 columns (BD Biosciences, Palo Alto, CA). The concentration of the purified RNA was determined spectrophotometrically at an optical density at 260 nm and adjusted to 10^2 to 10^7 copies/5 ml with TE (Tris-EDTA) buffer containing 0.25 U/ml of RNase inhibitor and 5 mM dithiothreitol. The RNAs were then stored at −20°C until use.

Primers, probe, and internal control for the detection of *M. tuberculosis* complex by TRC method. Synthetic oligonucleotides used for the TRC reaction included a pair of amplification primers (designated the promoter primer [5'-AAT TCT AAT ACG ACT CAC TAT AGG GAG ACG GAA AGG TCT CTT CGG AGA TAC-3'] and the antisense primer [5'-ACA AGA CAT GCA TCC CGT-3']), a scissors probe (5'-TTT CCG TTC GAC TTG CAT GTG TTA-3') to initiate the TRC reaction, and an INAF probe (5'-CGA AGT GCA GGG C*AG ATC, where the asterisk indicates the base position linked by oxazole yellow) to detect the RNA amplicons. For the specific detection of MTC, primers were designed to amplify base positions 313 to 443 of *M. tuberculosis* 16S rRNA (GenBank accession no. Z83862). As shown in Fig. 2, oxazole yellow-linked and ethidium bromide-linked INAF probes were synthesized for the homogeneous and simultaneous detection of the target 16S rRNA and the internal amplifica-